



THESIS TF 142520

THE INVESTIGATION OF ELECTRONEGATIVITY FUNCTIONAL GROUP EFFECTS ON MALEIMIDE ELECTROLYTE ADDITIVE IN LITHIUM ION BATTERY

GIYANTO
2413 202 003

Supervisor :
Prof. Fu-Ming Wang
Dr. -Ing. Doty Dewi Risanti, S.T., M.T.

MASTER DOUBLE DEGREE PROGRAM
RENEWABLE ENERGY ENGINEERING
DEPARTMENT OF ENGINEERING PHYSICS
FACULTY OF INDUSTRIAL TECHNOLOGY
INSTITUT TEKNOLOGI SEPULUH NOPEMBER
SURABAYA
2016

Tesis disusun untuk memenuhi salah satu syarat memperoleh gelar
Magister Teknik (M.T.)

di

Institut Teknologi Sepuluh Nopember

oleh:

GIYANTO

NRP. 2413 202 003

Tanggal Ujian: 19 Juli 2016

Periode Wisuda: September 2016

Disetujui oleh:

1. Dr.-Ing. Doty Dewi Risanti, S.T., M.T.  (Pembimbing)
NIP: 19740903 199802 2 001

Direktur Program Pascasarjana,

an. Direktur Program Pascasarjana
Asisten Direktur

Prof. Dr. Ir. Iri Wicajaja, M.Eng.
NIP. 19611021 198603 1 001

Prof. Ir. Djauhar Manfaat, M.Sc., Ph.D.
NIP. 19601202 198701 1 001



“This page intentionally left blank”



M10322801

Thesis Advisor: Fu-Ming Wang



碩士學位論文指導教授推薦書
Master's Thesis Recommendation Form

Department : Graduate Institute of Applied Science and Technology

Student's Name: GIYANTO GIYANTO

Thesis title: The investigation of electronegativity functional group effects on
maleimide electrolyte additive in lithium ion battery

This is to certify that the thesis submitted by the student named above, has been
written under my supervision. I hereby approve this thesis to be applied for
examination.

Advisor: Fu-Ming Wang

Co-advisor:

Advisor's Signature:

Date: 2016 / 7 / 19 (yyyy/mm/dd)

“This page intentionally left blank”



M10322801

Thesis Advisor: Fu-Ming Wang

碩士學位考試委員會審定書

Qualification Form by Master's Degree Examination Committee

Department: Graduate Institute of Applied Science and Technology

Student's Name: GIYANTO GIYANTO

Thesis Title:

The investigation of electronegativity functional group effects on maleimide electrolyte additive in lithium ion battery

This is to certify that the dissertation submitted by the student named above, is qualified and approved by the Examination Committee.

Degree Examination Committee

Members' Signatures:

Fu Ming Wang
Chorngshyan Chen

Jung-Mu, Hsu

Advisor:

Fu Ming Wang

Program Director's Signature: _____

Department/Institute Chairman's Signature: _____



Date: 2016 / 7 / 19 (yyyy/mm/dd)

“This page intentionally left blank”

Abstract

This research studies the electronegativity functional group effects on maleimide-based electrolyte additives to the solid electrolyte interface (SEI) formation on the graphite anode. Two maleimide compounds with the electronegativity functional groups as substituent, 4-flouro-o-phenylenedimaleimide (F-MI) and 4-cyano-o-phenylenedimaleimide (CN-MI) have been successfully synthesized. 1M LiPF_6 in ethylene carbonate (EC): propylene carbonate (PC): di-ethylene carbonate (DEC) (3:2:5 in volume) containing 0.1 wt % of F-MI and CN-MI additives can provide higher electrochemical stability and higher reversibility capability. The presence of the electronegativity functional group (F and CN) was found that the SEI layer formation is used to suppress the decomposition electrolyte within higher reduction potential at 2.35 to 2.33 V vs. Li/Li^+ . The cells with F-MI and CN-MI additives provide lower charge-transfer resistance and higher ionic diffusivity in comparison with commercial product (O-MI) and blank electrolyte. In addition, scanning electron microscopy (SEM) and energy dispersive X-ray spectroscopy (EDX) analysis were also conducted in order to understand the effects of additive on the morphology of the MCMB electrode surface. Our results show that F-MI and CN-MI additives are the most suitable additives due to its excellent SEI formation and battery performance enhancement compares with blank electrolyte and commercial product (O-MI).

Keyword: solid electrolyte interface, electronegativity functional group, maleimide-based additive, lithium ion battery

“This page intentionally left blank”

摘要

本研究目的在於用帶電負性官能基團之馬來酰亞胺電解液添加劑其對於石墨負極的固體電解質界面 (SEI) 生成影響作探討。兩種馬來酰亞胺生成物有著電負性官能基團之取代物成功地被合成出來，分別為：4-flouro-o-phenylenedimaleimide(F-MI)以及 4-cyano-o-phenylenedimaleimide(CN-MI)。一體積莫爾濃度之 LiPF_6 在體積比為 3:2:5 的碳酸乙烯酯(EC):碳酸丙烯酯(PC):碳酸二乙烯(DEC)下添加 0.1 wt% 的 F-MI 跟 CN-MI 添加劑，可以提供更高的電化學穩定性以及更佳的可逆性能力。電負性官能基團 (F 以及 CN) 被發現其 SEI 層的生成可以被用來抑制在較高的還原電位 2.35 到 2.33 伏特(相對於 Li/Li^+)所造成的電解質分解問題。和商業的電池(O-MI)以及空白對照組的電池做比較，利用 F-MI 跟 CN-MI 添加劑所組成的電池提供了較低的電荷轉移之電阻和較高的離子擴散速率。除此之外，也透過掃描型電子顯微鏡(SEM)和能量色散 X 射線光譜儀(EDX)分析來研究兩種添加劑對於 MCMB 電極表面形態所造成的影響。我們的結果發現，本實驗之添加劑其良好的 SEI 生成以及與商業的電池(O-MI)跟空白對照組相比之電池性能的提高，此兩種添加劑為最適當的添加劑。

關鍵字：固體電解質界面、電負性官能基團、馬來酰亞胺添加劑、鋰離子電池。

“This page intentionally left blank”

Acknowledgement

Firstly, I would like to express my deepest gratitude to “**Allah SWT**” for all His blessing and mercy, I can finish my thesis and get my Master Degree.

This thesis would not have been accomplished without the support from the several people. The foremost, I would like to express my highest gratitude and thank for Professor Fu-Ming Wang for his patient, guidance, time, support, and reminders for the past two years as my advisor. I would also like to acknowledge to Prof. Chorng-Shyan Chern and Dr. Jung-Mu Hsu for their advice, inputs, and critics that assist to improve this thesis.

Thank you for my grandmother “Mbah Banem”, my mother Ngadinem, my father Ngatno, my brother Syam, my sister Eny, and my fiancé Ari Nur Alfiyah for the support, motivation, and never ending love for me until now, I won’t be who I am now without you all. Moreover, to my lab mates, Hendra, Fauzan, Sylvia, Nadia, Rion, Roy, Cindy, Candy, Lester, and Steven, thank you for the warmest welcome and friendship since the first time I came into the Lab, I had so much joy and happiness with you guys. For Wafa, Ukik, Sasongko, Bang Riona, Bang Andri, Faisal, Riza, Ulza, and everyone that I can’t mention one by one, thank you for being my family in Taipei and thank you for the support and motivation for last two years.

Surabaya, January 2017

Giyanto

“This page intentionally left blank”

Table of Contents

Approval Sheet.....	i
Master's Thesis Recommendation Form	iii
Qualification Form by Master's Degree Examination Committee	v
Abstract	vii
摘要.....	ix
Acknowledgement	xi
Table of Contents	xiii
List of Figures	xv
List of Tables.....	xvii
CHAPTER I INTRODUCTION	1
1.1 Background	1
1.2 Problems Formulation	4
1.3 Research Purposes.....	4
CHAPTER II LITERATURE REVIEW	5
2.1 Lithium Ion Battery Components.....	5
2.2 Solid Electrolyte Interface (SEI)	15
2.3 SEI Modification	27
2.4 Electrolyte Additives	36
2.5 Maleimide-based Additive	42
2.6 The Electronegativity Functional Group Effect on Electrolyte Additive.....	44
CHAPTER III RESEARCH METHODOLOGY	47
3.1 Research Design.....	47
3.2 Materials.....	49
3.3 Equipments.....	50
3.4 Experimental Procedure	51
CHAPTER IV RESULT AND DISCUSSION	57
4.1 Characterization of New Additives	57
4.2 Electrochemical Analysis	61
4.3 SEI Evaluation.....	74
CHAPTER V CONCLUSION.....	79
REFERENCE.....	81

“This page intentionally left blank”

List of Figures

Figure 2.1: Crystal structures of three classes of the cathode materials.....	6
Figure 2.2: Schematic representation of the chemical composition of the SEI layer at the graphite (a); Illustration of stepwise formation of SEI layer (b).	16
Figure 2.3: A possible pathway for reduction mechanism of the organic carbonate solvent (EC-based) on the graphite anode.....	18
Figure 2.4: Surface layer deposited on the graphite particles (a), deposit layer showing cracks (b).....	22
Figure 2.5: SEM micrographs showing deposit surface layer resulting from a breakdown of the SEI layer on pristine graphite (a); cycling condition (b).....	25
Figure 2.6: Schematic diagram showing the SEI interaction with the electrolyte leading to the various interactions.....	26
Figure 2.7: Schematic diagrams of the solid-electrolyte-interface (SEI) layer formed at the surface of bare graphite and the composites of graphite selectively deposited with metals: (a) Bare graphite and (b) Composite with metal.	29
Figure 2.8: SEM images of (a) unmodified and (b) carbon-coated NG.....	30
Figure 2.9: Mechanism of SEI formation by LiBOB, (a) semi-carbonate species formation, (b) oligomeric borate formation	34
Figure 2.10: Illustration of the basic way to improve the performance of graphite electrodes by the use of electrolyte additives.	37
Figure 2.11: General mechanism of polymerization additives.	38
Figure 2.12: The main possible of VC degradation product.	39
Figure 2.13: Reduction reaction mechanism of FEC which lead to the formation of polymeric species.	41
Figure 2.14: Reaction mechanism of reaction type additives.	41
Figure 2.15: Chemical structure of phenylenedimaleimide positional isomers.....	43
Figure 2.16: Chemical structure of additives containing electronegativity and electron withdrawing functional groups.	44
Figure 3.1: Flow chart of research design.	48
Figure 3.2: F-MI synthesis mechanism.....	51
Figure 3.3: CN-MI synthesis mechanism.....	51
Figure 3.4: Reaction mechanism of hydrogenation part.	52

Figure 3.5: Reaction mechanism of dehydration part.....	53
Figure 3.6: Schematic Arrangement of Coin Cell Assembly.	54
Figure 4.1: Mass spectral of F-MI.....	57
Figure 4.2: ¹ H NMR of N,N'-o-phenylenedimaleimide (O-MI).	58
Figure 4.3: ¹ H NMR of 4-fluoro-phenylenediamaleimide (F-MI).	58
Figure 4.4: Mass spectral of CN-MI.	59
Figure 4.5: ¹ H NMR of cyano-phenylenediamaleimide (CN-MI).	60
Figure 4.6: Cyclic voltammograms of lithium plating/stripping on the anode half-cell with different electrolyte.	62
Figure 4.7: Charge and discharge profile of MCMB/Li half-cell with and without additives under 0.1 C-Rate at the room temperature and potential range 0-3 V vs Li/Li ⁺ , (a) 1 st cycle (b) 2 nd cycle.	64
Figure 4.8: Comparison of cycle-ability of MCMB/Li half-cell with and without additives in electrolyte under 0.1 C-rate at room temperature and potential range 0-3 V vs Li/Li ⁺ , (a) charge (b) discharge capacity.	66
Figure 4.9: Charge and discharge profile of MCMB/LiCoO ₂ full-cell with and without additives at 1 st cycle under 0.1 C-Rate at the room temperature and potential range 3 - 4.2 V vs Li/Li ⁺	67
Figure 4.10: Comparison of cycle-ability of MCMB/LiCoO ₂ full-cell with and without additives until 20 th cycles at room temperature and potential range 3 - 4.2V vs Li/Li ⁺ , (a) charge (b) discharge capacity.....	68
Figure 4.11: Rate capability of MCMB/LiCoO ₂ full-cell with and without additives at room temperature and potential range 3 - 4.2V vs Li/Li ⁺	69
Figure 4.12: Equivalent-circuit for the EIS of Li/graphite cell. The EIS was recorded at 0.05V.	70
Figure 4.13: Impedance Spectra of MCMB/Li half-cell after tenth cycle with 1 M LiPF ₆ and EC:PC:DEC (3:2:5 v/v) electrolyte system.....	71
Figure 4.14: Impedance Spectra of MCMB/LiCoO ₂ full-cell after tenth cycle with 1 M LiPF ₆ and EC:EMC (1:1 v/v) electrolyte system.	73
Figure 4.15: SEM image of MCMB before electrochemical cycling (x500). Inset shows image at x3000 magnification.....	75
Figure 4.16: SEM image of MCMB/Li half cell after the tenth cycles (x500) in cell with additive electrolyte (a) Blank, (b) O-MI, (c) F-MI and (d) CN-MI.	75
Figure 4.17: EDX profile of MCMB/Li half-cell after the tenth cycles in cell with additive electrolyte (a) Blank, (b) O-MI, (c) F-MI and (d) CN-MI.....	76
Figure 4.18: Graphic of chemical content of MCMB surface selected regarding EDX profile of variant MCMB with electrolyte additive.	77

List of Tables

Table 2.1: Characteristics of three classes of the cathode materials.	6
Table 2.2: Advantages and disadvantages of the cathode materials.	7
Table 2.3: The major advantages and disadvantages of the cathode materials.	9
Table 2.4: Properties of the solvents are commonly used in LIBs applications	13
Table 2.5: Salts used in electrolytes system for LIBs applications.	14
Table 2.6: Possible reduction reactions of alkyl carbonate solvents.	19
Table 2.7: List of known chemical compounds formed on the surface of carbon/graphite SEI layers	23
Table 2.8: The chemical structures of MI-based additives and the oxidation potentials measured from HOMO, LUMO orbital energies.	42
Table 4.1: Reduction potential peak of MCMB/Li ⁺ anode half-cell.	63
Table 4.2: Electrode kinetic parameters obtained from equivalent circuit fitting of experimental data with various electrolytes in MCMB/Li half-cell. .	71
Table 4.3: Electrode kinetic parameters obtained from equivalent circuit fitting of experimental data with various electrolytes in MCMB/LiCoO ₂ full-cell.	73

“This page intentionally left blank”

CHAPTER I

INTRODUCTION

1.1 Background

The limited of fossil fuel resources and the fears of an energy crisis have caused the rapid increase in development of an alternative and sustainable energy source, such as wind, wave and solar. However, energy generation from these technologies requires an energy storage device that rechargeable with high efficiency for feasibility and reliability. Therefore, the rechargeable battery is the most suitable and important device for energy storage system and energy conversion system. Since commercialized by Sony in the early 1990s, lithium ion batteries (LIBs) has becomes one of the most popular types of rechargeable battery for electronic portable devices due to their high energy and power density, lack of memory effect, high stability, high charge and discharge rate capabilities, high operating voltage, low self-discharge rate, light weight, small size, low cost, long life cycle, and high efficiency compared to other commercial battery technologies (Park, Zhang et al. 2010, Jeong, Kim et al. 2011, Choi, Chen et al. 2012). Moreover these types of LIBs applications are currently extended to electric vehicles and power storage system for power grids.

Along with the expansion of LIBs applications, some requirements such as higher specific energy and power, longer life cycle, higher stability, lower cost and safety must be met by the batteries (Jeong, Kim et al. 2011, Choi, Chen et al. 2012). In electric vehicle applications, for example, the battery should have high energy density for driving range and have high power rate for acceleration. While in power storage system applications, the battery is not too demand higher energy and power densities, because it's applications not affected by volume or weight. However, the battery should demonstrate longer battery lifetime and lower cost. In addition, some other problem in development of LIBs technology that are currently the main concern is the thermal stability and safety issues, which is caused by thermal runaway and can further degrade battery performance. Hence, in order to meet the demand of the global market, especially in electric vehicle

and power storage applications, intensive efforts had been made worldwide to developing of LIBs technology.

In order to develop better LIBs, it is essential to recognize the basics of how a lithium-ion battery works. In an ideal LIBs reaction mechanism, lithium ions are reversibly shuttled between the cathode and the anode with 100% efficiency and no side reactions occur during the charge/discharge process. However in practice, the efficiency (commonly called “columbic efficiency”) is slightly lower than 100%, and several surface side reactions between the electrolyte and electrode occur during normal operation of the cell or under abnormal conditions (elevated temperature and overcharge). For example, lithium ions can react with the electrolyte decomposition and forming a solid electrolyte interface (SEI) layer composed of lithium salts. These side reactions have several negative effects on the battery performance such as: increase the energy barrier for the charge-transfer reaction at the electrode surface, decrease active surface area of the electrode, and reduce reversibility. Moreover, fire or explosion which caused by thermal runaway also can be occur if the battery is operated at elevated temperatures or under abuse conditions.

Generally, LIBs performance can be improved by enhanced electrical conductivities and ionic diffusivities on the electrode materials (anode and cathode) and increased ionic conductivities on the electrolyte (Park, Zhang et al. 2010). Many studies have been reported in developing new materials for anode (Goriparti, Miele et al. 2014) (oxide, phosphate), cathode (Fergus 2010) (different graphite type, alloys, and carbon based compound), separator (Lee, Yanilmaz et al. 2014) and electrolyte (organic, solid state, and ionic liquid) (Song, Wang et al. 1999, Stephan 2006, Ghandi 2014, Marcinek, Syzdek et al. 2015). One of the most economic and effective methods for the improvement of LIBs performance is use of electrolyte additives (Zhang 2006). Adding a small amount of additives to the electrolyte could lead to prolonged cycle life and improved battery safety (Zhang, Huang et al. 2014). The role of these additives is expected to facilitate a better electrochemical performance of the LIBs. Electrolyte additives can produce electrochemical reactions that lead to a formation of a stable interface between the electrode and electrolyte in the lithium-ion battery system. This interface

(commonly called “SEI layer”) is one of the most important factors for enhancing the battery performance because that is where most reactions occur, including intercalation/de-intercalation of lithium ions and electrolyte decomposition.

There are a lot of additives, such as: vinylene carbonate (VC), vinyl ethylene carbonate (VEC), fluoroethylene carbonate (FEC), ethylene sulfite (ES), and maleimide (MI) have been proposed to be a promising additives in LIBs application. MI-based additive is one type of additives which has been developed by Wang et al. It has been proven (Wang, Cheng et al. 2009), that this additive is capable to enhance the rate capability and cycle-ability due to its low LUMO energy, high reductive potential and unique reaction mechanism compared with alkyl carbonate, such as EC, PC, and DEC. In addition, Wang et al. also conducted several studies such as: combining MI-based additive with H₂O as binary additive (Cheng, Wang et al. 2012) and studying the effect of isomer positional MI-based additive (Wang, Yu et al. 2013), discovering the next generation of MI-based additive which can improve the performance of the SEI layer.

Several studies reported that the SEI layer formed by the electrolyte additives is dependent on the functional group incorporated. The additives containing electron withdrawing functional groups such as fluorine (F) and cyanide (CN), and chlorine (Cl) could make the compound more electrophilic, facilitate reduction mechanism and increase polymerization reaction (Whittingham 2004, Haregewoin, Leggesse et al. 2014). Previous research reported that the modification of propane sultone (PS) made by introducing an electron withdrawing fluorine group, showed better performance compared with PS and vinylene carbonate (VC) commercial additive in a LiCoO₂/graphite cell (Jung, Park et al. 2013). The presence of the fluorine functional group can enhances the anodic stability and cathodic reactivity of the additive which helps to improve its SEI forming ability.

Both of fluorine and cyanide is an electron withdrawing functional groups elements that have a high electronegativity. The molecule with the higher electronegativity and stronger electron withdrawing substitution believed can attract electron on lower LUMO, which decreases the energy band gap to early reduce and generate more effective and stable SEI layer. Previously, Hamidah et

all. studied the fluorine electron withdrawing group effect on MI-based compounds as electrolyte additive and discover excellent electrochemical performance of LIBs, especially at cycled test and high temperature application (Hamidah 2013). This study uses fluorine (F) and cyanide (CN) as substituent to investigate the electronegativity functional group effects on MI-based compounds that were used as an electrolyte additive in LIBs application. Hopefully, the new MI-based additive can facilitate a highly stable SEI formation and subsequently can enhance the battery performance.

1.2 Problems Formulation

Based on the background that was described in the previous sub-section, the problems formulation of this research are to:

1. How to synthesize 4-flouro-phenylenedimaleimide (F-MI) and 4-cyano-phenylenedimaleimide (CN-MI) as the new MI-based additive by combining the attractive properties of MI-based additives and high electronegativity functional group (F and CN). In this research, the commercial additive o-phenylene-dimaleimide (o-MI) and blank electrolyte (without any additive) will be used as comparison.
2. How to investigate the SEI formation phenomena of the battery cells with 3 kinds of MI-based additives related to the presence of substituent and electronegativity effect and its effect to the battery performance.

1.3 Research Purposes

Based on the background and problem formulation that was described above, the purpose of this research are to:

1. Synthesize 4-flouro-phenylenedimaleimide (F-MI) and 4-cyano-phenylenedimaleimide (CN-MI) as the new MI-based additive by combining the attractive properties of MI-based additives and high electronegativity functional group (F and CN).
2. Investigate the SEI formation phenomena of the battery cells with 3 kinds of MI-based additives related to the presence of substituent and electronegativity effect and its effect to the battery performance.

CHAPTER II

LITERATURE REVIEW

2.1 Lithium Ion Battery Components

2.1.1 Cathode

In LIBs application, cathode or positive electrode materials serves as source of Li^+ ions during intercalation processes. Generally, cathode materials are made from oxides compounds based on transition metals which can release lithium ions from the structure by oxidation of the transition metal cations (Whittingham 2004). Most of the cathode materials have a layered structure, with transitional metal ions ordered in a layer (slab) and lithium ions in the following layer (inter-slab). There are several requirements which must be met by cathode material to be a good candidate for positive electrode materials in LIBs applications, such as:

1. The cathode materials should be high in both of Li^+ ion diffusivity and electrical conductivity to keep high power density.
2. The cathode materials also should have high potential relative to Li/Li^+ reference electrode to enable high operating voltage.
3. The material structure should be able to incorporate with large amount of lithium to provide higher energy density.
4. The structural changes during cycling should be as small as possible in order to give high reversibility and long life cycle.
5. The materials should be inexpensive, low toxic, high safety, and easy to be synthesized.

Based on the crystal structures, the cathode materials can be divided into three classes: layered, spinel, and olivine (Figure 2.1). Layered materials are used as cathodes for high-energy systems, while spinel oxides and olivines are considered in the case of high-power LIBs due to their low cost and long-life requirements, respectively (Fergus 2010, Xu, Dou et al. 2013, Julien, Mauger et al. 2014).

Table 2.1 summarizes the electrochemical properties of the three classes of cathode materials. Currently, LiCoO_2 is one of the most commonly used cathode material in commercial LIBs application due to its high working voltage, structural stability and long cycle life (Xu, Dou et al. 2013). However, LiCoO_2 has several disadvantages, such as: high cost, low reversibility, toxic, and poor in safety. Several researchers have devoted their big effort to search an alternative material of cathode, such as: layered materials ($\text{LiNi}_{0.8}\text{Co}_{0.15}\text{Al}_{0.05}\text{O}_2$ or NCA and $\text{LiNi}_{1/3}\text{Co}_{1/3}\text{Mn}_{1/3}\text{O}_2$ or NMC), spinel materials (LiMn_2O_4 and variants), and olivine materials (LiFePO_4 and $\text{LiFe}_{1/2}\text{Mn}_{1/2}\text{PO}_4$). The major advantages and disadvantages of cathode materials except LiCoO_2 are summarized in Table 2.2.

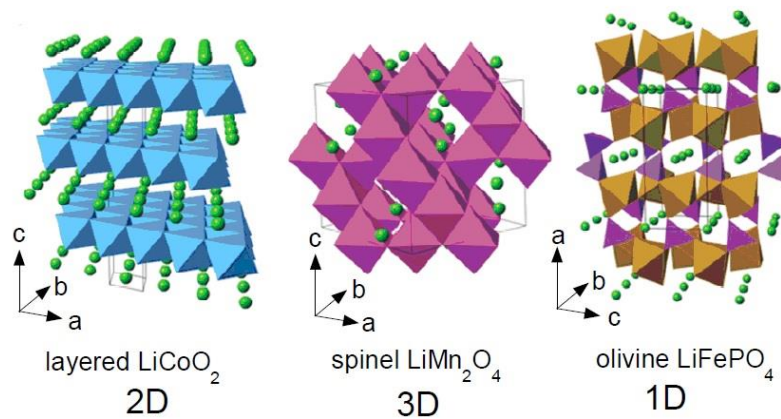


Figure 2.1: Crystal structures of three classes of the cathode materials (Julien, Mauger et al. 2014)

Table 2.1: Characteristics of three classes of the cathode materials

Structure	Material	Specific capacity ^a (mAh/gr)	Average potential (V vs. Li/Li^+)
Layered	LiCoO_2	272 (140)	4.2
	$\text{LiNi}_{1/3}\text{Mn}_{1/3}\text{Co}_{1/3}\text{O}_2$	272 (200)	4.0
Spinel	LiMn_2O_4	148 (120)	4.1
	$\text{LiMn}_{3/2}\text{Ni}_{1/2}\text{O}_4$	148 (120)	4.7
Olivine	LiFePO_4	170 (160)	3.45
	$\text{LiFe}_{1/2}\text{Mn}_{1/2}\text{PO}_4$	170 (160)	3.4/4.1

^a Value in parenthesis indicates the practical specific capacity of the electrode.
Source: (Julien, Mauger et al. 2014)

Table 2.2: Advantages and disadvantages of the cathode materials

Advantages	Disadvantages
NMC ($\text{LiNi}_{1/3}\text{Co}_{1/3}\text{Mn}_{1/3}\text{O}_2$) and variants	
<ul style="list-style-type: none"> - High capacity - High operating voltage - Slow reaction with electrolytes - Moderate safety (oxygen release) 	<ul style="list-style-type: none"> - High cost of Ni and Co - Potential resource limitations - Relatively new in performance - Controlling patents
NCA ($\text{LiNi}_{0.8}\text{Co}_{0.15}\text{Al}_{0.05}\text{O}_2$)	
<ul style="list-style-type: none"> - Performance is well established - Slow reaction with electrolytes - High capacity - High voltage - Excellent high rate performance 	<ul style="list-style-type: none"> - High cost of Ni and Co - Potential resource limitations
LMO (LiMn_2O_4) and variants	
<ul style="list-style-type: none"> - Low cost - Excellent high rate performance - High operating voltage - No resource limitations - Moderate safety (oxygen release) 	<ul style="list-style-type: none"> - Mn solubility issue, affecting cycle life - Low capacity
LFP (LiFePO_4 and variants)	
<ul style="list-style-type: none"> - Moderately low cost - Excellent high rate performance - No resource limitations - Very slow reaction with electrolyte - Excellent safety (no oxygen release) 	<ul style="list-style-type: none"> - Low operating voltage - Low capacity, especially for substituted variants - Controlling patents

Source: (Doeff 2013)

2.1.2 Anode

The anode or negative electrode acts as recipient of Li^+ ions during intercalation process and acts as electron donors during de-intercalation process. There are several basic requirements that must be met by anode materials, such as: (i) the potential of lithium insertion and extraction in anode relative to Li/Li^+ reference must be as low as possible; (ii) the anode materials should be able to accommodate as high as possible amount of lithium ions to achieve high specific energy; (iii) the anode structure should endure against repeated lithium insertion and extraction without any structural damage to obtain high reversibility and long life cycle; and (iv) low cost, high safety, and easy for fabrications (Wu, Rahm et al. 2003, Goriparti, Miele et al. 2014).

The first generation of the anode material for LIBs application is lithium metal (lithium foil). Even though lithium metal becomes one of the highest capacity among anode materials (3860 mAh/gr), safety issues prevent the use of lithium metal as anode material in rechargeable LIBs (Goriparti, Miele et al. 2014). When lithium metal is used as anode material, lithium is often deposited in a dendrite form during intercalation and de-intercalation processes. These lithium dendrites are porous, have high surface area, and very reactive in organic electrolyte. The growth of dendrites formation on the lithium metal could lead to short circuit, fire, and explosion. Therefore, this issue has driven researchers to find alternative anode materials for rechargeable LIBs application.

At present, a lot of anode materials have been investigated including carbon based (soft and hard), titanium-based oxides, alloys/de-alloys materials, and conversion materials like transition metal oxides (Table 2.3). However, carbon based anode, especially graphitic carbon (graphite) is one of the most widely used anode materials due to its excellent features, such as flat and low working potential vs. lithium, low cost and good cycle life (Goriparti, Miele et al. 2014). Graphite allows the intercalation of only one Li-ion with six carbon atoms, with a resulting stoichiometry of LiC_6 corresponding to a theoretical specific capacity of 372 mAh/gr (850 mAh/cm³). However, graphite also has several disadvantages, such as: low diffusion coefficient which makes it have a limit in application (low power density LIBs application) and the carbon material also can easily react with non- aqueous electrolytes, especially at elevated temperatures, to provide undesired reactions which can cause material degradation and reduce reversibility capacity. Currently, carbon based anode materials are still under intensive development to improve their performance, especially in term of specific capacity and life cycle. Recent development on modifying carbon anode materials have been reported, including mild oxidation of graphite, forming the composites with metals and metal oxides, and coating by polymers and other kinds of carbons (see Chapter 2.2).

Table 2.3: the major advantages and disadvantages of the cathode materials

Anode materials	Specific capacity (mAh/gr)	Advantages	Disadvantages
Carbon based			- Low coulombic efficiency
- Hard carbon	200-600	- Good working potential	- High voltage hysteresis
- Carbon Nano Tubes (CNTs)	1116	- Low cost	- High irreversible capacity
- Graphene	780/1116	- Good safety	
Titanium oxides		- Extreme safety	- Very low capacity
- LiTi_4O_5	175	- Good cycle life	- Low energy density
- TiO_2	330	- Low cost	
		- High power capability	
Alloys/de-alloys			- Low coulombic efficiency
- Silicon	4212	- High capacity	- Unstable SEI formation
- Germanium	1624	- High energy	- Large potential hysteresis
- Tin	993	- Low cost	- Poor cycle life
- Antimony	660	- Environmentally compatibility	
- Tin oxide	790		
- SiO	1600		
Conversion materials		- High specific capacity	- Poor capacity retention
- Metal oxides	500-1200	- Low operation potential and low polarization	- Short cycle life
- Metal phosphides /nitrides/sulfides	500-1800		- High cost of production

Source: (Goriparti, Miele et al. 2014)

Another category of anode materials such as tin oxide (LiTi_4O_5 and TiO_2), tin-based alloys/de-alloys (Si, Ge, SiO, SnO_2), and conversion materials (metal oxides/phosphides/nitrides/sulfides) also still under development by researchers in order to meet the larger market of the commercial LIBs, especially for electric vehicles and power storage applications. Tin-based oxide materials are very good candidates for application in high power LIBs due to the high reversible capacity, high power density and high safety. However these materials show low electronic conductivity, low theoretical capacity and poor energy density. On the contrary, tin-based alloy/de-alloy materials can provide higher capacities and higher energy density than graphite and tin-based materials. Nevertheless, these materials have a major drawback in term of cycle life due to the high volume expansion /contraction and the larger irreversible capacity at the initial cycles. While

conversion materials are still far away from the large commercial LIBs market, due high volume expansion, poor electron transport, and poor capacity retention (Goriparti, Miele et al. 2014).

2.1.3 Electrolyte

Electrolyte materials separate anode and cathode and play a significant role on transmitting electrons and lithium ions during charging and discharging processes. Electrolyte is one of the key components that define the LIBs performance such as: charge and discharge rate capabilities, safety, cycle-ability, and current density. The main requirement for the electrolyte is therefore that it must have a wide electrochemical stability window, should provide an ionic conduction path between the cathode and the anode (ionic conductor), and should assure electronic separation of the electrodes in order to avoid short circuit between them (electronic insulator). In addition, there are also some important characteristics that must be owned by an electrolyte such as: high chemical and electrochemical stability, non-reactivity with the electrode materials to prevent side reactions between electrodes and electrolyte, high boiling and low melting points to prevent the solidification at low temperature and explosion at high temperature, high safety, low toxicity and low cost. Currently, there are 3 types of electrolytes have been used in LIBs application. These are: liquid electrolyte system (solution of lithium salt in a polar, organic, aprotic solvent), polymer electrolyte (Marcinek, Syzdek et al. 2015).

Most of commercial LIBs are designed based on liquid electrolytes, containing a lithium salt dissolved in organic alkyl carbonate solvent. Both of the lithium salt and organic solvents have the effects which determine the ionic conductivity and electrochemical stability of the electrolyte. Therefore, the suitable choice of the salt and solvent is one of the most important criteria in the design of the LIBs application. In some cases, an amount of additives are added to the mixture of the lithium salt and solvent as electrolyte additives that is useful for facilitating SEI formation and preventing degradation of the active material caused by solvent co-intercalation (Xu 2010, Marcinek, Syzdek et al. 2015).

2.1.3.1 Solvent

An appropriate solvent for LIBs application should have some addition criteria such as: high lithium ion conductivity, a wide electrochemical stability window, high dielectric constant, low viscosity, and good solubility to be able to dissolve on the salt. The suitable solvents for LIBs application are mainly chosen from two families of organic compounds, namely ethers and esters. Ethers are more reduction resistant and esters are more stable against oxidation. Table 2.4 shows the structure and physical properties of the solvents that are commonly used in LIBs application. Among them, the organic di-esters of carbonic acid or carbonates from esters family deserve more attention since they possess high dielectric constant and low viscosity. Ethylene carbonate (EC) is usually selected as a primary solvent when graphite is used as an anode material. It offers ability to protect the surface of the graphene structure during cycling and provide a sufficient high conductivity (Marcinek, Syzdek et al. 2015). Although EC is the most preferred solvent in LIBs application, but it is a solid at room temperature. It is therefore commonly needs to be modified or mixed with one or more other solvent which has a lower conductivity in order to enhance their low temperature performance. Propylene carbonate (PC) has many advantages over other organic carbonates for being use in the battery electrolyte, such as: lower cost and better low temperature performance. However, the use of PC in LIBs has been problem due to extensive co-intercalation of solvent molecules along with lithium ion into the graphite and subsequently can causes severe exfoliation of graphitic carbon electrodes (Choi, Chen et al. 2012, Shkrob, Zhu et al. 2013).

2.1.3.2 Lithium Salt

Lithium salts are added to the solvents to act as charge carries of the current passed in the lithium cell during the electrochemical process. Generally, lithium salt having a large anion is chosen to facilitate anion-cation dissociation. An excellent lithium salt must meet several requirements, such as: high solubility, high ionic conductivity, high electrochemical and thermal stability, low toxicity, and good safety properties (Xu 2010, Marcinek, Syzdek et al. 2015).

The most common lithium salt used in the electrolyte is lithium hexafluorophosphate (LiPF_6). It gives high ionic conductivities in carbonate based solvents, and shows excellent cycling properties at room temperature. However, it is well known that LiPF_6 is easily decomposed even at room temperature and produces the strong of lewis acid base PF_5 (Agubra 2014). These decomposition products could be reacted with the moisture traces (H_2O) and produce acid HF. Even, the side product (HF) and H_2O impurities also can reacts with the electrolyte and SEI components, to form a various species that the major product from these reactions is LiF. As we know that LiF is an unwanted SEI component and contrary to lithium carbonates due to its low permeability for Li^+ ions. The LiF species from these reactions with Li_2CO_3 are deposited on the electrode as passivation layer (commonly called solid electrolyte interphase (SEI) and eventually lead to poor ionic conductivity and degrade battery performance.

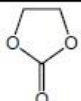
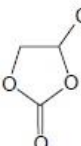
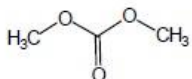
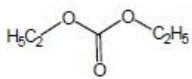
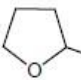
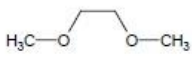
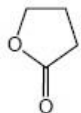
Other commonly used salts are LiClO_4 ; LiAsF_6 ; LiBF_4 ; ($\text{LiB}(\text{C}_2\text{O}_4)_2$), commonly called LiBOB; LiCF_3SO_3 , commonly called LiTF; ($\text{LiN}(\text{CF}_3\text{SO}_2)_2$), commonly called LiTFSI; and ($\text{LiN}(\text{SO}_2\text{C}_2\text{F}_5)_2$), commonly called LiBETI. The salts properties commonly used in LIBs applications are listed in Table 2.5. These salts might have some advantages and disadvantages compared to LiPF_6 . LiClO_4 has low interfacial resistance, low cost, stable at ambient temperature and ease of synthesis, but it gives poor safety due to high oxidizability of anions (ClO_4^-) and explosive at high temperature (Xu 2010, Marcinek, Syzdek et al. 2015). LiAsF_6 is poisonous because it contains arsenic. However, the SEI layer formed on the anode surface is very stable during cell operation. LiBF_4 is very similar and cheaper material than LiPF_6 , less toxic than LiAsF_6 , and better safety than LiClO_4 . Nevertheless it is less hygroscopic and lower ionic conductivity due to the low dissociation constant. These salts are designed for special purpose, such as for high temperature LIBs applications. LiBOB salt has many advantages compared to LiPF_6 including high thermal stability, good safety, and more stable SEI layer. However, these salts have lower ionic conductivity, especially at temperatures below 0°C , lower rate capability due to higher internal resistance, and show inconsistent performance because of impurities in the LiBOB salt. LiTFSI exhibits an interesting ionic conductivity in carbonate solvent but it has a strong

corrosion behavior at the Al current collector and expensive. Whereas LiBETI is more stable and no Al corrosion below 4.4 V.

2.1.3.3 Additives

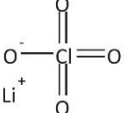
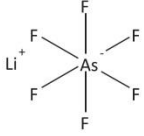
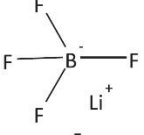
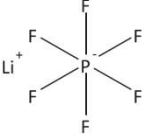
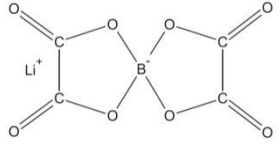
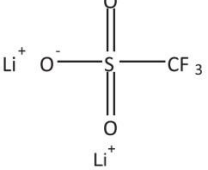
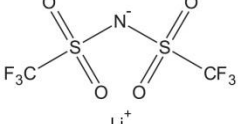
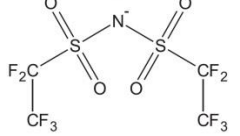
Electrolyte can be modified by adding some additives into electrolyte system to stabilize SEI as well as improve anode performance. Adding additive is an effective and economic method for modifying SEI layer and improved electrochemical performance. Generally, the amount of additive in the electrolyte is no more than 5% either by weight or by volume while its presence significantly improves the cycle-ability and cycle life of LIBs (Zhang 2006).

Table 2.4: Properties of the solvents are commonly used in LIBs applications

<i>Solvent name and abbrev.</i>	<i>Structural fomula</i>	<i>Melting point (°C)</i>	<i>Boiling point (°C)</i>	<i>Dielectric constant, ϵ</i>
Ethylene carbonate, EC		39-40	248	89.6 (40°C)
Propylene carbonate, PC		-49	240	64.4
Dimethyl carbonate, DMC		4.6	91	3.12
Diethyl carbonate, DEC		-43	126	2.82
2-Methyl-tetrahydrofuran, 2Me-THF		-137	79	6.29
Dimethoxy ethane, DME		-58	85	7.20
γ -Butyrolactone, γ-BL		-43	204	39.1

Source : (Marcinek, Syzdek et al. 2015)

Table 2.5: Salts used in electrolytes system for LIBs applications

Salt	Structure	Solvent	Ionic conductivity (S.cm ⁻¹)
LiClO ₄		PC EC/DMC	5.6 8.4
LiAsF ₆		PC EC/DMC	5.7 11.1
LiBF ₄		PC EC/DMC	3.4 4.9
LiPF ₆		PC EC/DMC	5.8 10.7
LiBOB		EC/DMC	7.5
LiTF		PC	1.7
LiTFSI		PC EC/DMC	5.1 9.0
LiBETI		N/A	N/A

Source : (Marcinek, Syzdek et al. 2015)

2.2 Solid Electrolyte Interface (SEI)

Solid electrolyte interface (SEI) is the passivation layer formed on the graphite anode during first cycle (more than 80%) and less in cathode. SEI layer is one of the most important factors for determining the battery performance, including cycle life, rate capability, columbic efficiency, irreversible capacity, thermal stability and safety. The SEI layer is a Li^+ conductor but an insulator to electron flow and serves as a protective film for solvent co-intercalation that may lead to electrode exfoliation. In addition, an excessive formation of SEI is highly undesirable due to it consumes a considerable amount of lithium ions, decrease the active area of the electrode, increase interfacial resistance and eventually leading to an irreversible capacity loss. Moreover, fire or explosion which caused by thermal runaway and further SEI formation also can be occur if the battery is operated at elevated temperatures or under abuse conditions. For all of these reason, it is crucial to understand the fundamentals of the SEI formation, including the formation mechanism, structure, chemical composition, morphology, and its correlation to the electrochemical performance of LIBs. There are several requirements that must be met by the SEI to be categorized as an effective and a good SEI passivation layer (Zhang, Ding et al. 2001, Verma, Maire et al. 2010, Agubra and Fergus 2014, An, Li et al. 2016), such as:

1. SEI formation kinetics should be fast, allowing it to form completely before onset of Li^+ intercalation. In other words, or SEI formation potential should be more positive than Li^+ intercalation potential.
2. It should be compact, stable, uniform and adhesive deposit on the electrode material and also insoluble in the electrolyte even at high temperature.
3. It should be possess a good ionic conductivity and a good electronic insulator.
4. It should be elastic and flexible to accommodate non-uniform electrochemical behavior.

2.2.1 SEI Formation Mechanism

As described above, most of the SEI passivation layer formed on the graphite anode as a result decomposition of the electrolyte components (solvent and salt), and mainly during the first cycle. These salts and solvents are reduced earlier at potential ($< 0.8 \text{ V}$ vs Li/Li^+) that is higher than the intercalation potential of lithium ions, resulting in the precipitation of various species on the surface of the graphite anode to form the SEI passivation layer (Fig.2.2b). The SEI layer is a thin layer composed of two or more layers with a thickness of about 30-50 nm, and mainly consist of organic and inorganic compounds many others including oligomeric and polymeric compounds (Fig.2.2a). The first layer typically is a thin and dense layer that is rich in inorganic compounds such as LiF , Li_2O , Li_2CO_3 and close to the electrode surface. These inorganic compounds are unwanted product due to insulators to both Li^+ ions and electrons. While the following layers are thicker, loose and porous that is rich in organic compounds or polymer compounds such as lithium ethylene di-carbonate (Li_2EDC) and contact with electrolytes (Zhang, Ding et al. 2001, Verma, Maire et al. 2010, Agubra and Fergus 2014, Soto, Ma et al. 2015, An, Li et al. 2016).

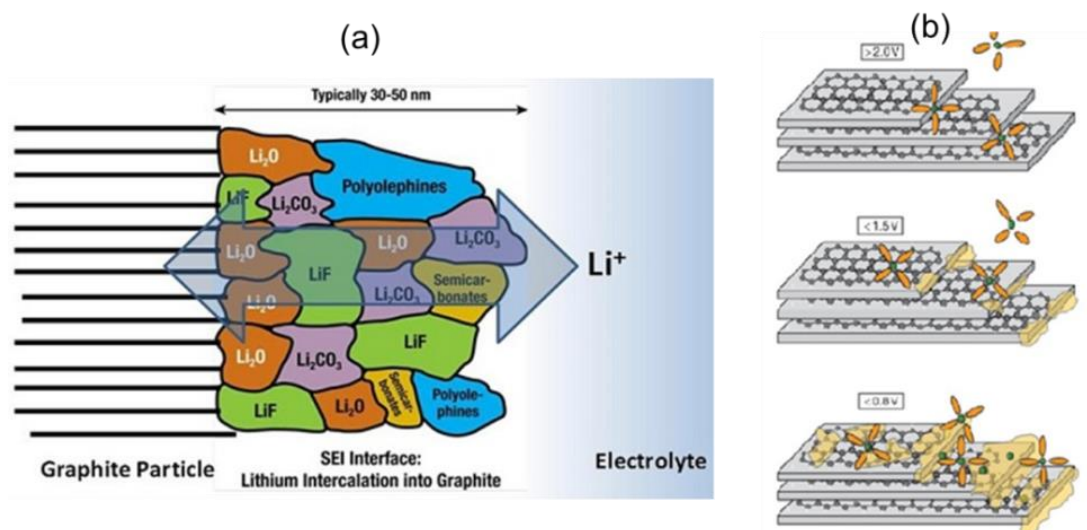


Figure 2.2: (a) Schematic representation of the chemical composition of the SEI layer at the graphite; (b) Illustration of stepwise formation of SEI layer (Choi, Chen et al. 2012)

There are various reduction processes that compete with each other on the carbon/graphite surface during charging. The reactants are solvents, salts, additives, and trace air impurities (such as H_2O). Electrochemical reaction rates differ depending on their intrinsic properties such as: reductive potential, reduction activation energy, and exchange current density. They also depend on reaction sites (basal or edge), pre-decomposed precipitate sites, and many other different anode surface conditions. In addition, temperature, concentration of electrolyte salt, and reduction current rate also significantly affect SEI formation as well. Therefore, it is very difficult to identify and analyze the SEI formation mechanism when all of these variable conditions are mixed together (An, Li et al. 2016).

2.2.2 Solvent Reduction Mechanism

Generally, it has been accepted that the SEI formation is a two-step process. During the first step when the graphite electrode is polarized, the components in the organic electrolyte undergo reductive decomposition to form new chemical species. In the second step, these decomposition products undergo a precipitation process and begin forming the SEI layer until all the sites on the graphite surface are covered. Even though several studies have been conducted to understand the formation mechanism of the SEI layer, it has been a major topic of debate and remains unclear, especially for solvent reduction mechanism.

Aurbach and co-workers have made the most marked contribution in identifying the SEI formation reaction mechanism and effective chemical constituents in SEI layer. They argued that the organic solvents are limited to be reduced on the surface of the graphite anode to form an intermediate radical anion, and then decomposition of the radical anion is expected to produce the constituents of the SEI layer. An organic solvent (EC-based) reduction process generally involves the solvent molecules, a transfer of one or two electron, and amount of Li^+ to produce a lithium carbonate species (Li_2CO_3), lithium alkyl carbonate species ($(\text{CH}_2\text{OCO}_2\text{Li})_2$) and a gas (C_2H_4). These reaction products would be deposited quickly on the graphite anode surface as a SEI layer that can prevent electron transfer, further decomposition, and electrode exfoliation.

Sometimes other reduction products, such as lithium alkoxides or lithium oxalates also have been found, but these are believed to be minor product of the solvent reduction. A possible pathway for reduction mechanism of the organic carbonate solvents (EC-based) on the graphite anode is shown in Fig.2.3 (Zhang 2006, Shkrob, Zhu et al. 2013, Agubra and Fergus 2014).

Another type of solvents commonly used in electrolyte system is PC-based solvent. The reduction mechanism of PC based electrolyte solvents is generally similar with EC based electrolyte solvents and it produces polymerized carbonate species, such as: Li_2CO_3 , $\text{CH}_3\text{CH}(\text{OCO}_2\text{Li})\text{CH}_2\text{OCO}_2\text{Li}$, and propylene gas (C_3H_6). The reduction products of PC-based solvent contain loose and unstable alkyl tails in the form of methyl groups, which do not cohesively adhere to the anode surface and causes exfoliation of the graphite anode. The proposed major reduction paths of the solvents used in LIBs are summarized in Table 2.6.

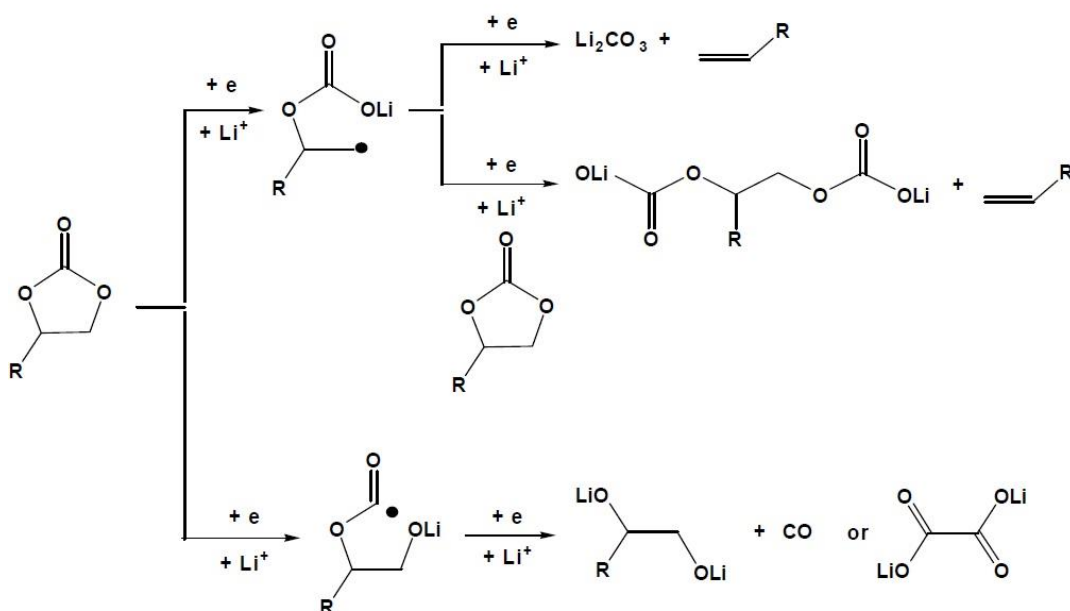


Figure 2.3: A possible pathway for reduction mechanism of the organic carbonate solvent (EC-based) on the graphite anode (Xu 2010)

Table 2.6: Possible reduction reactions of alkyl carbonate solvents

Solvent	Possible reduction reaction mechanism
EC	$(\text{CH}_2\text{O})_2\text{CO} + 2\text{e}^- + 2\text{Li}^+ \rightarrow \text{Li}_2\text{CO}_3 \downarrow + \text{C}_2\text{H}_4 \uparrow$
	$2((\text{CH}_2\text{O})_2\text{CO}) + 2\text{e}^- + 2\text{Li}^+ \rightarrow (\text{CH}_2\text{OCO}_2\text{Li})_2 \downarrow + \text{C}_2\text{H}_4 \uparrow$
	$2((\text{CH}_2\text{O})_2\text{CO}) + 2\text{e}^- + 2\text{Li}^+ \rightarrow ((\text{CH}_2)_2\text{OCO}_2\text{Li})_2 \downarrow$
PC	$\text{CH}_3\text{C}_2\text{H}_3\text{O}_2\text{CO} + 2\text{e}^- + 2\text{Li}^+ \rightarrow \text{Li}_2\text{CO}_3 \downarrow + \text{C}_3\text{H}_6 \uparrow$
	$2(\text{CH}_3\text{C}_2\text{H}_3\text{O}_2\text{CO}) + 2\text{e}^- + 2\text{Li}^+ \rightarrow \text{CH}_3\text{CH}(\text{OCO}_2\text{Li})\text{CH}_2\text{OCO}_2\text{Li} \downarrow + \text{C}_3\text{H}_6 \uparrow$
EMC	$\text{CH}_3\text{CH}_2\text{O}(\text{C}=\text{O})\text{OCH}_3 + \text{e}^- \rightarrow \text{CH}_3\text{CH}_2\text{O}(\text{C}^* - \text{O}^-)\text{OCH}_3$
	$\text{CH}_3\text{CH}_2\text{O}(\text{C}^* - \text{O}^-)\text{OCH}_3 + \text{e}^- + 2\text{Li}^+ \rightarrow \text{LiO}(\text{C}=\text{O})\text{CH}_3 + \text{CH}_3\text{CH}_2\text{OLi}$
DMC	$\text{CH}_3\text{OCO}_2\text{CH}_3 + 2\text{e}^- + 2\text{Li}^+ \rightarrow \text{Li}_2\text{CO}_3 \downarrow + \text{C}_2\text{H}_6 \uparrow$
	$\text{CH}_3\text{OCO}_2\text{CH}_3 + \text{e}^- + \text{Li}^+ \rightarrow \text{CH}_3\text{OCO}_2\text{Li} \downarrow + \text{CH}_3$
	$\text{CH}_3\text{OCO}_2\text{CH}_3 + \text{e}^- + \text{Li}^+ \rightarrow \text{CH}_3\text{OLi} \downarrow + \text{CH}_3\text{CO}_2$
DEC	$\text{CH}_3\text{CH}_2\text{OCO}_2\text{CH}_2\text{CH}_3 + \text{e}^- + \text{Li}^+ \rightarrow \text{CH}_3\text{CH}_2\text{OCO}_2\text{Li} \downarrow + \text{CH}_3\text{CH}_2$
	$\text{CH}_3\text{CH}_2\text{OCO}_2\text{CH}_2\text{CH}_3 + \text{e}^- + \text{Li}^+ \rightarrow \text{CH}_3\text{CH}_2\text{OLi} \downarrow + \text{CH}_3\text{CH}_2\text{CO}_2$

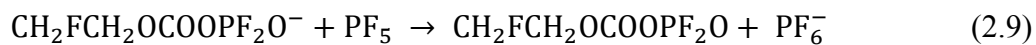
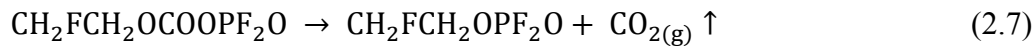
Source: (Zhang, Ding et al. 2001, Shkrob, Zhu et al. 2013, Agubra and Fergus 2014, Soto, Ma et al. 2015, An, Li et al. 2016)

2.2.3 Salt Decomposition

Besides solvents reduction, electrolyte salts also are reduced to some extent during charging and produce inorganic species (LiF , Li_2SO_3 , Li_3N) that also precipitates on the surface of the electrode. As described before that the most common electrolyte salt used in LIBs application is LiPF_6 . The decomposition of LiPF_6 follows a two-step process in which the decomposition is related to the release of free acid followed by decomposition of the salt. The initial reaction for the salt decomposition is electron transfer from the electrode to the salt molecule to produce a toxic alkyl-fluoro-phosphate (PF_5) where it can trigger autocatalytic process due to the presence of impurities (H_2O , CO_2 , or alcohol) in the cell system. The stability of PF_5 in solution depends on the solvent, it is stable in polar sterically compact solvents, such as EC, while in less polar and bulky solvents such as DMC and DEC, the PF_5 species is often unstable. Thus, the

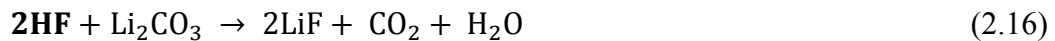
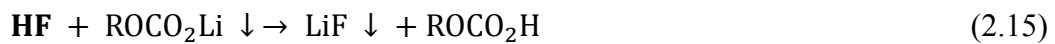
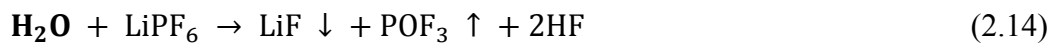
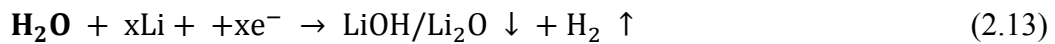
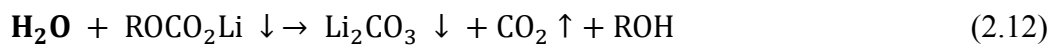
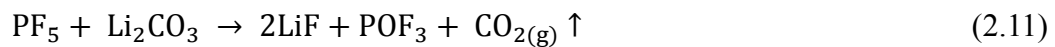
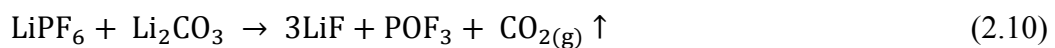
decomposition of LiPF_6 is further promoted by solvents with large dielectric constants and high viscosity, such as EC. Solvents with high dielectric constant can increase the ionization of the salt and accelerates its reduction reaction and its subsequent reaction with water to form the LiOH species (Agubra and Fergus 2014, Nie and Lucht 2014, An, Li et al. 2016).

The LiPF_6 salt decomposes into LiF and the lewis acid PF_5 or a Li^+ and the anion PF_6^- as shown in Eq. 2.1 and 2.2. The dissociated of lewis acid PF_5 can react with H_2O (Eq. 2.3 and 2.4), existing as an impurity in solution or the alcohol to form POF_3 , or PF_4OH and species HF . The species PF_4OH also can further dissociate to produce POF_3 and HF that remain in solution (Eq. 2.5). Furthermore, the decomposition species of POF_3 will react with carbonate solvents (EC) and/or anion PF_6^- to produce a various and complex species and also initiated autocatalytic process which in this case is highly undesirable (Eq. 2.3 – Eq. 2.9) (Agubra and Fergus 2014).



The LiPF_6 salt which is thermodynamically unstable can react with Li_2CO_3 from EC reduction to produce LiF , POF_3 and CO_2 (Eq. 2.10 and 2.11). Even, the side product from salt decomposition such as HF species and H_2O impurities also can reacts with the electrolyte and SEI components, to form a various species that the major product from these reactions is LiF . As we know that LiF is an unwanted SEI component and contrary to lithium carbonates due to its low

permeability for Li^+ ions. The LiF species from these reactions with Li_2CO_3 are deposited on the electrode and form an insoluble, non-uniform and electronically insulating layer on the graphite particle surfaces. Important reactions involving H_2O and HF impurities are shown in Eq. 2.12 – Eq. 2.18. It is therefore crucial to keep the impurities content in the electrolyte to minimum levels, especially for H_2O content. In addition, the content of HF species also must be kept at a low level due to it can cause metal ion dissolution from cathode materials and destroys SEI layer formed on the carbon-based anodes, thus having a detrimental impact on the performance and safety of battery.



In addition, SEI layers also easily react with ambient CO_2 and H_2O to form inorganic lithium-containing compounds such as Li_2CO_3 and Li_2O . For example, ROCO_2Li and ROLi react with CO_2 to form Li_2CO_3 . The lithium in the SEI will also react spontaneously with atmospheric oxygen to form various lithium oxides (Li_2O , Li_2O_2 and LiO_2). These oxides are strong nucleophiles and react further with organic solvents and semi-carbonates to form carbonates and alkoxides. All of these reaction products (LiF , Li_2CO_3 , LiOH and Li_2O) on the electrode surface may crack (Fig 2.4) due to the differences in the coefficients of thermal expansion between the deposit layer and the graphite particles. This phenomenon could allow further reaction at these newly created crevices on the electrode surface and subsequently leads to exfoliation of the graphite electrode (Agubra and Fergus 2014, An, Li et al. 2016).

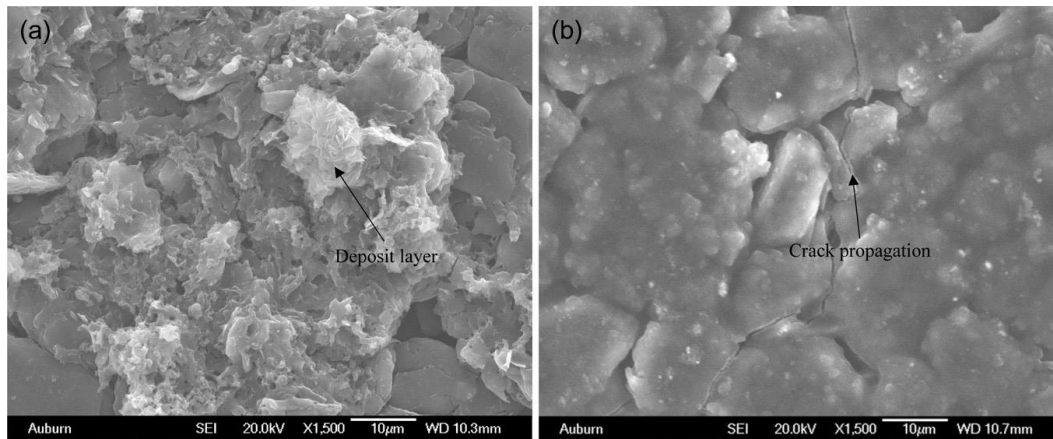


Figure 2.4: (a) surface layer deposited on the graphite particles, (b) deposit layer showing cracks (Agubra and Fergus 2014)

2.2.4 SEI Features, Morphology, and Chemical Composition

The chemical composition on the SEI layer is a highly debated subject. According to the above reactions, it has been agreed that the SEI layer formed on the graphite anode surface is generally derived from partial or complete reduction products of the electrolyte system (solvent and salt). As described before that the most commonly chemical products of the SEI layer is dominated by inorganic compounds such as LiF , Li_2O and Li_2CO_3 which formed close to the graphite surface, and organic compounds or polymer compounds such as ROCO_2Li and $(\text{CH}_2\text{OCO}_2\text{Li})_2$ which formed further out towards the electrolyte. Table 2.7 provides a through list of the most agreed upon compounds found in the SEI on graphite anodes (Verma, Maire et al. 2010, An, Li et al. 2016). The chemical composition and morphology of the SEI are affected not only by the electrolyte system, but also by the characteristic of the electrode materials such as: surface properties of the electrode (surface area, particle shape, size and distribution, etc.) and structure of the electrode (type of binder, binder content, porosity, mechanical properties, etc.).

Table 2.7: List of known chemical compounds formed on the surface of carbon/graphite SEI layers

SEI Component	Notes
$(\text{CH}_2\text{OCO}_2\text{Li})_2$	Being a two electron reduction product of ethylene carbonate (EC); it is found mostly in the SEI of the EC based electrolytes.
ROCO_2Li	They are present in the outer layer of the SEI. They occur in most PC containing electrolytes, especially when the concentration of PC in the electrolyte is high.
Li_2CO_3	It may also appear as a reaction product of semi-carbonates with HF, water, or CO_2 .
ROLi	Most commonly found in the SEI formed in ether electrolytes like tetrahydrofuran (THF), but may also appear as DMC or ethyl methyl carbonate (EMC) reduction product. It is soluble and may undergo further reactions.
LiF	Mostly found in electrolytes comprising of fluorinated salts like LiAsF_6 , LiPF_6 , LiBF_4 . It is a major salt reduction product. HF contaminant also reacts with semi-carbonates to give LiF by product. Amount of LiF increases during storage.
Li_2O	It may be a degradation product of Li_2CO_3 during Ar^+ sputtering in the XPS experiment.
LiOH	It is mainly formed due to water contamination. It may also result from reaction of Li_2O with water or with aging.
Polycarbonates	Present in the outermost layer of the SEI, close to the electrolyte phase. This part imparts flexibility to the SEI.
$\text{Li}_2\text{C}_2\text{O}_4$	It is found to be present in 18,650 cells assembled in Argonne National Laboratory containing 1.2 M LiPF_6 in EC:EMC(3:7) electrolyte. Li carboxylate and Li methoxide were also found in their SEI.
HCOLi	It is present when methyl formate is used as co-solvent or additive.
HF	It is formed from decomposition LiPF_6 and the water in the solvents. It is highly toxic and can attack components of the cell.

Source: (Verma, Maire et al. 2010, An, Li et al. 2016)

Basically, the layer structure of the graphite anode consists of two kinds of surfaces, prismatic (edge) surfaces and basal plane surfaces. The SEI layer formed at the graphite basal plane differs in morphology and chemical composition from that formed at the edge plane. The SEI formed at the basal plane does not need to have ionic conductivity, but it does need to be electronically insulating and impermeable to other electrolyte components. Ideally, basal plane surfaces are homogeneous, smooth and consist of only carbon atoms (organic compounds). In contrast, the prismatic surfaces are heterogeneous, rough, and apart of carbon mainly contain various, mostly oxygen-containing surface groups (inorganic compounds). It is well known that the prismatic and basal plane surface areas of graphite show a different physical, chemical and electrochemical behavior in many things. Graphite electrode materials with high crystallinity, low defect concentration, low amount of prismatic surfaces and less surface impurity represent low surface reactivity towards the electrolyte can obtain large reversible capacity and long electrode cycle life (Verma, Maire et al. 2010, Agubra and Fergus 2014, An, Li et al. 2016).

2.2.5 The Growth of SEI Layer

It is accepted that the growth of the SEI layer also affects to the battery performance. The SEI layer should be remains stable in any conditions. In facts, the chemical composition, thickness, structure, and morphology of the SEI layers do not stay constant during cycling and can transform to be another species due to many factors such as: partial electrolyte decomposition, volume expansion or contraction of the electrode materials, and operation conditions (temperature and electrochemical condition). For example in the graphite anode cases at normal operation, these transformation processes usually take place very quickly so that the overall system remains stable. However under abuse conditions (elevated temperature and overcharge), the growth of the SEI layer will be abnormal and under controlled due to an undesired side reaction between graphite anode and SEI, or SEI and the electrolyte, or graphite anode and the electrolyte. These excessive reactions are highly detrimental for the performance of LIBs including irreversible capacity, cycle-ability, rate capability, and safety.

An ineffective SEI layer is a source for trapped solvated lithium ions in the growing SEI layer which can lead to the formation of metallic lithium clusters. The trapped solvated Li ions will react with the electrolyte to produce reduction species and significantly increases the charge transfer resistance. The accumulated reduction species on the graphite surface decrease the pore size in SEI layer and that leads to a sluggish Li^+ intercalation/de-intercalation kinetics (Agubra and Fergus 2014).

The constituent of the SEI layer also can react with the trace of impurities (H_2O) to generate an auto-catalyzer (OPF_2OR) and subsequently accelerate the decomposition of the salt that alters SEI layer composition and distorts its structure. This structural change in the SEI layer decreases its ion conductivity at cell storage conditions (Fig. 2.5). At high cell operating temperatures and charge rate, the SEI completely breaks down structurally leading to many degradation mechanisms such as exfoliation and amorphization occurring at the graphite/electrolyte interface. The interaction of the SEI layer with its surroundings from its formation stage to its eventual degradation is depicted in Fig 2.6. On the other hand, a robust and effective SEI layer inhibits further solvent decomposition, prevents solvent co-intercalation, prevents graphite exfoliation and improves cycling efficiency. In addition, an effective SEI layer will reduce significantly the double layer capacitance and increases ionic conductivity in the electrode/electrolyte interface (Agubra and Fergus 2014).

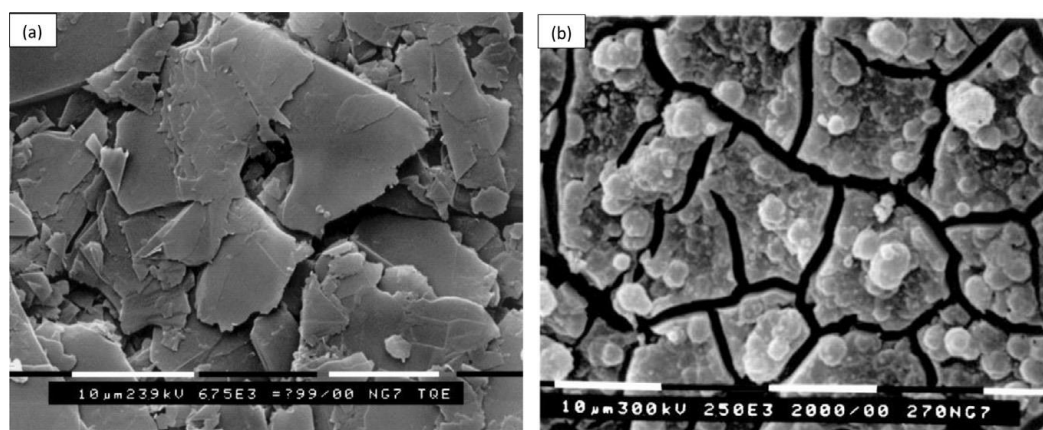


Figure 2.5: (a) SEM micrographs showing deposit surface layer resulting from a breakdown of the SEI layer on pristine graphite; (b) cycling condition (Agubra and Fergus 2014)

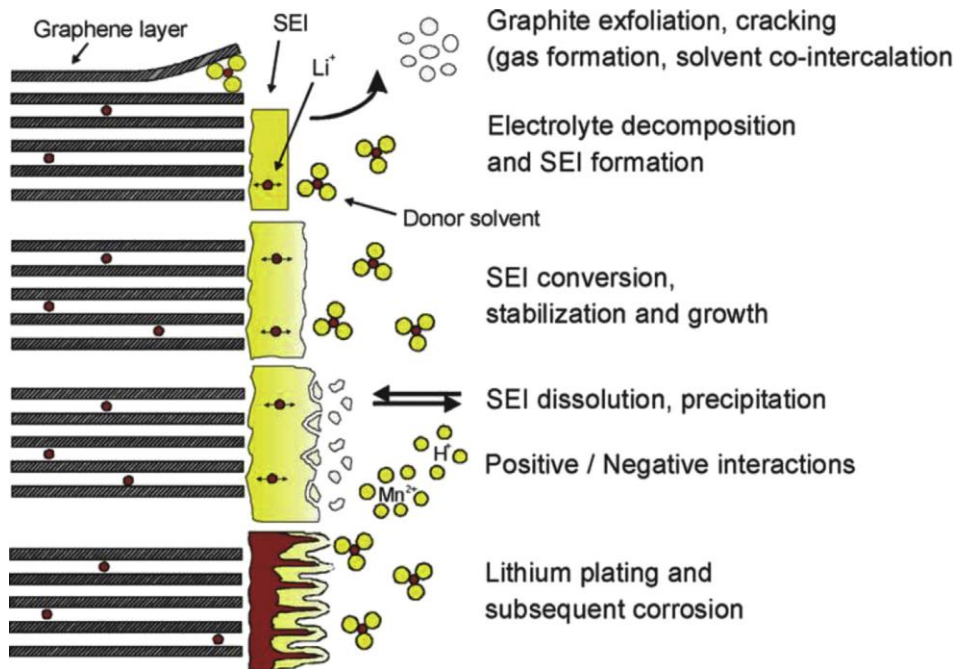


Figure 2.6: Schematic diagram showing the SEI interaction with the electrolyte leading to the various interactions (Agubra and Fergus 2014)

2.2.6 Characterization of SEI Layer

As described above, the characteristic of the SEI layer is very difficult to be clearly identified and highly dependent on the type of electrolytes and the characteristics of the electrode materials. A large variety of tools and techniques have been used for analyzing SEI layer, including formation mechanism, morphology, structure, and chemical compound of SEI layer. Traditional electrochemical methods such as electrochemical impedance spectroscopy (EIS) and cyclic voltammetry (CV) have been used to studying the thickness and evolution of the SEI layer. EIS is a non-destructive analysis tool, which provides useful information from a complex electrochemical system having a diffusion layer, electrolyte resistance, electrode kinetics, and double-layer capacitance. To diagnose EIS spectra properly, a good equivalent circuit model is required. CV has also been successfully implemented to understand the SEI formation by measures current in the anodic (oxidation) and cathodic (reduction) directions. In addition, electrochemical quartz crystal microbalance (EQCM) also could be implemented to study the dynamic of electrolyte decomposition during reduction

process, combine with linear sweep voltammetry (LSV) (Zhang, Xu et al. 2006, Zhang 2007, Cheng, Wang et al. 2012, Radvanyi, Van Havenbergh et al. 2014, Tsai, Taberna et al. 2014, Wang and Rick 2014, Torres, Cantoni et al. 2015).

Because the SEI is a thin layer on the electrode surface, several surface characterization techniques such as Fourier transformed infrared spectroscopy Raman spectroscopy (FT-IR), X-ray photoelectron microscopy (XPS), scanning electron microscopy (SEM), and transmission electron microscopy (TEM) are required to identify the chemical compounds, structure, and morphology of the SEI layer (Chattopadhyay, Lipson et al. 2012, Malmgren, Ciosek et al. 2013, Shkrob, Zhu et al. 2013, Cresce, Russell et al. 2014, Park, Shin et al. 2014, Shi, Zhao et al. 2014, Shi, Ross et al. 2015).

2.3 SEI Modification

In order to get a better SEI layer, several researches have been applied various methods to develop the SEI properties, such as modifying the composition of the electrode materials, surface modification of the electrode materials, adding additive on the electrode materials, choosing the several solvent on the electrolyte, develop new lithium salt, adding additive into lithium salt, and adding additive into the electrolyte. In general, these modifications will be classified into three categories: surface modification on the anode materials, surface modification on the cathode materials, and modification on the electrolyte systems (Fu, Liu et al. 2006).

2.3.1 Surface Modification of the Anode Materials

Many researchers have indicated that the formation of the SEI layers are affected by morphology and chemistry of the graphite surface, and are associated with the catalytic activity which in this case is undesirable and detrimental to the electrochemical performance of LIBs. Recent development on modifying carbon anode materials as well as modifying the SEI layer on the anode surface have been reported, including mild oxidation of graphite, forming the composites with metals and metal oxides, and coating by polymers and other kinds of carbons. These modifications are expected to deactivate the catalytic activity of the fresh

graphite surface, decrease charge transfer resistance of the electrode, increase electronic conductivity, reduce side reactions between electrode and electrolyte related to the thickness of the SEI layer, increase in the number of host sites for lithium storage related to the reversibility capacity and also improve its electrochemical performance (Fu, Liu et al. 2006).

2.3.1.1 Mild Oxidation

It was first reported by Peled et.al. that mild oxidation of artificial graphite could modify its electrochemical performance as anode materials in LIBs. The main processes of the mild oxidation can be summarized as following: (1) removing some active sites (edge planes) and/or defects in graphitic materials resulting in improvement of surface structure; (2) forming a dense layer of oxides (carbonyl, carboxyl, hydroxyl) acting as an efficient passivation layer; (3) producing nanochannels and/or micropores acting as host sites, inlet, and outlet for reversible lithium storage. Several oxidation agents such as ozone, air and CO_2 have been reported to improve electrochemical performance of the anode materials including reversibility capacity, coulomb efficiency at first cycle, and cycle-ability. However, these methods are very difficult to control due to the oxidation process happens at the interface between the solid and the gas phase. In addition, the modification degree of these methods also depends on the graphite species and the oxidant agents. An aqueous solution such as: $(\text{NH}_4)_2\text{S}_2\text{O}_8$, HNO_3 , $\text{Ce}(\text{SO}_4)_2$, and H_2O_2 can also serve as liquid oxidant agents. These liquid oxidants are much better than gaseous oxidant due to it can be easily performed and provides materials with higher reversibility capacity. However each of these liquid oxidants also have some disadvantages, such as: both of $(\text{NH}_4)_2\text{S}_2\text{O}_8$ and HNO_3 has drawback that they are not friendly to the environment and $\text{Ce}(\text{SO}_4)_2$ resulting some corrosion of equipment due to introduction of a salt. While a solution of H_2O_2 is an effective oxidant agent since it can be recycled by electrolysis and do not produce detrimental effect to the environment.

2.3.1.2 Forming the Composites with Metals and Metal Oxides

Forming the composites by depositing metal and metal oxides on the anode surface is a good method to improve electrochemical performance of the anode materials. This method is used to prevent the exfoliation of the anode materials due to solvent co-intercalation, especially the electrolyte solution which contain propylene carbonate (PC) solvent (Fig 2.7). Several kinds of metal, such as: Ag, Al, Au, Bi, Cu, In, Ni, Pb, Pd, Sn, Zn have been reported able to increase the reversible capacity, rate capability, and cycle life of the graphite anode compared with the bare graphite (without metal composites). In addition, metal oxides, such as SnO , SnO_2 and MxO ($\text{M} = \text{Cu}$, Ni , Fe and Pb) can also be deposited onto the surfaces of the graphite anode, and these surface coatings can also act effectively. Electrochemical performance of the composites highly depends on the material deposited, the amount of material deposited, depositing method and heating treatment.

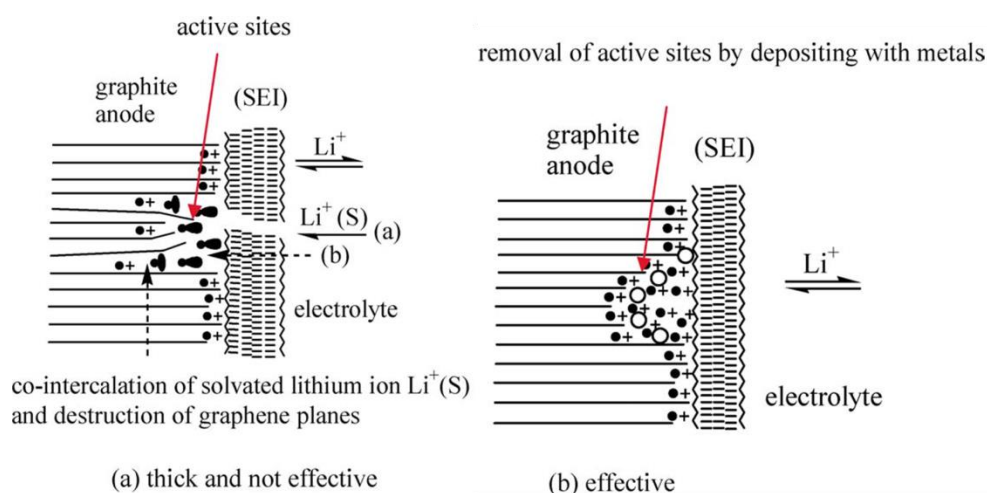


Figure 2.7: Schematic diagrams of the solid-electrolyte-interface (SEI) layer formed at the surface of bare graphite and the composites of graphite selectively deposited with metals: (a) Bare graphite and (b) Composite with metal NG (Fu, Liu et al. 2006)

2.3.1.3 Coating with polymers and other kinds of carbons

Coating with polymers and other kinds of carbons can also result in an improved performance of anode materials. The polymer coating, such as: polythiophene, polypyrrole, and polyaniline, decreases the contact of the active

sites of graphite with the electrolytes and subsequently enhances reversibility capacity. In addition, polymers have a good elasticity and also can act as ionic conductor. While carbon coating is commonly used to prevent exfoliation of the graphite anode. It is because the active sites on the graphite surface are covered by carbon coating and do not directly contact the electrolytes. Thus, the decomposition of electrolyte system is greatly reduced, and an effective SEI film is formed. Fig 2.8 shows SEM result of the unmodified natural graphite (NG) and the carbon-coated NG. Both graphite samples have similar shapes and particle sizes. However, the unmodified NG has rough and craggy surface, whereas the surface of the carbon-coated NG is smooth and shows no clear cracks.

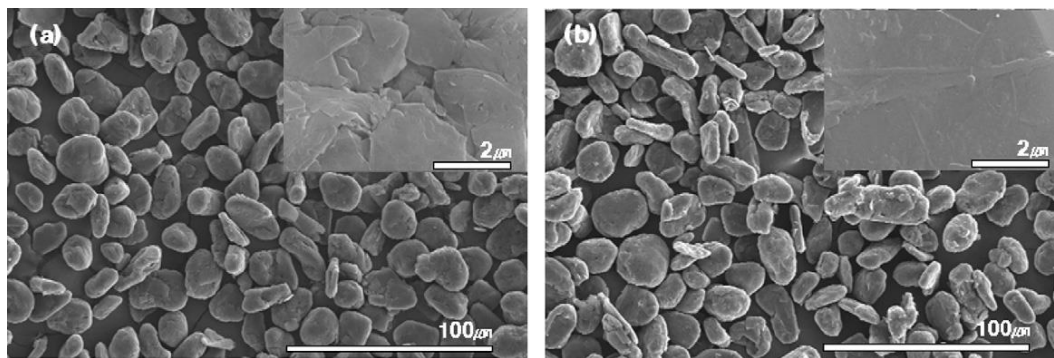


Figure 2.8: SEM images of (a) unmodified and (b) carbon-coated NG (Fu, Liu et al. 2006)

2.3.2 Surface Modification of the Cathode Materials

While much effort has been made in recent years to characterize the composition and properties of the SEI layer formed at the graphite-anode/electrolyte interface of the LIBs. However, in current LIBs technology, the cell voltage and capacities are mainly determined by the cathode material that is also the limiting factor for Li^+ transportation rate. LiCoO_2 is presently the most widely used cathode material available in the market due to it has a typical stable layered structure, high working voltage and long cycle life compared with other cathode materials such as: LiNiO_2 and spinel-type LiMn_2O_4 . Nevertheless LiCoO_2 also has several disadvantages, such as: high cost, low reversibility, toxic, and poor in safety. Hence, the developments of cathode materials become extremely crucial and received much attention in recent decades.

Generally, the performance of the cathode materials can be improved by two ways: doping by heteroatoms and surface coating onto surface of the cathode materials. Many heteroatoms such as: $\text{LiNi}_{0.8}\text{Co}_{0.15}\text{Al}_{0.05}\text{O}_2$ or NCA and $\text{LiNi}_{1/3}\text{Co}_{1/3}\text{Mn}_{1/3}\text{O}_2$ or NMC have been introduced able to enhanced electrochemical performance of the cathode material including enhance the charge-discharge rates, reduce the irreversible capacity loss in the first cycle, and increase the discharge capacity. In addition, surface coating also has been proven to be effective for improving the structural stability, capacity retention, rate capability, and even thermal stability of cathode materials. Several coating materials such as: MgO , SnO_2 , Al_2O_3 , ZrO_2 and other compounds has been reported can be coated onto the surface of LiCoO_2 as well as able to improve electrochemical performance of the electrode materials. The key mechanisms have been proposed to explain the positive effect of surface coating on the performance of cathode materials including the following:

1. Electron-conducting media that facilitates the charge transfer at the surface of particles;
2. Modification of cathode surface chemistry that improves performance;
3. HF scavenger that reduces the acidity of non-aqueous electrolyte and suppresses metal dissolution from the cathode materials;
4. A physical protection barrier that impedes the side reactions between cathode materials and non-aqueous electrolytes.

Similar with the surface modification on the anode materials, the electrochemical performance of the cathode materials also highly depends on the material coated, the amount of material deposited, depositing method and heating treatment. Coating with a thin layer of MgO onto the surface of LiCoO_2 presents two effects. Firstly, the surface coating itself acts as a protective layer to prevent a direct contact of the active core material with the electrolyte solution and decreases the dissolution of Co^{4+} - ions and then Mg^{2+} - ions from the MgO -coating can diffuse into the inter-slab space of the lattice, which suppresses the phase transition by occupying the left vacant Li^+ sites and prevents a vacancy disorder at high charge potentials. As a result, this surface modification improves the structural stability of LiCoO_2 without decreasing its available specific capacity.

SnO₂ coating can be performed by a sol–gel method and the properties of the coated LiCoO₂ depend on the following heat treatment. When a heat treatment temperature (HTT) is below 600 °C, Sn is mainly distributed on the surface and the coated LiCoO₂ exhibits an excellent structural stability and increase retention capacity. In contrary, Sn distributes uniformly throughout the coated LiCoO₂ particles and shows a capacity loss when the HTT is 600 °C. The effects of Al₂O₃ coating are also dependent on HTT. At a HTT of 700 °C, a solid solution LiCo_{1-x}Al_xO₂ is present on the surface of LiCoO₂ beyond 50 nm, and no evident improvement has been observed. If the HTT is below 700 °C, the solid solution LiCo_{1-x}Al_xO₂ mainly exists on the surface of LiCoO₂ particles within 50 nm. The high concentration of Al atoms at the particle surface region leads to the enhancement of structural stability of LiCoO₂ during cycling and also result in the same effects as the SnO₂-coating, without decreasing its available specific capacity and excellent in capacity retention. Besides the above mentioned metal oxides, LiMn₂O₄ also can be coated onto LiCoO₂ and the main consideration is to improve the safety problem of lithium ion batteries.

2.3.3 Modification on the Electrolyte System

As described in previous section, the most common electrolyte system for LIBs application use non-aqueous electrolyte which consists of Li-salts (LiPF₆) dissolved in an organic solvent (alkyl carbonate). Both of the lithium salt and organic solvents have the effects which determine the ionic conductivity and electrochemical stability of the electrolyte systems. Therefore, the suitable choice of the salt and solvent is one of the most important criteria in the design of the LIBs application. Hence, intensive efforts have been proposed to improve the electrochemical performance of electrolyte system, such as modifying electrolyte by adding some additive and creating new solvents and salts.

2.3.3.1 Salt Modification

State-of-the-art commercial lithium ion batteries use LiPF₆ as the electrolyte salt due to its superior properties when compared to other salts such as LiBF₄ and LiClO₄ (Zhang 2006). However as described in previous section, it has

problems related to thermal stability and reaction with moisture, which leads to the formation of LiF and PF_5 . In the presence of trace H_2O impurities, PF_5 undergoes hydrolysis at elevated temperatures producing HF which leads to transition metal dissolution from the cathode material. In the absence of H_2O , PF_5 also can react with the SEI components on the graphite and degrade the battery performance.

Some of the methods employed to minimize the thermal instability of the salt LiPF_6 , include inhibiting the transesterification of dialkylcarbonate and lowering the concentrations of protic impurities of H_2O and alcohol in the carbonate solvents. Another way to solving these problems related to the thermal stability of LiPF_6 is to use inorganic compounds, such as tris (2,2,2-trifluoroethyl) phosphite (TTFP) and low concentration of Lewis bases such as; triethylenediamine (TEDA), 2,2'-bipyridine (BIPY), triphenylphosphine (TPP) tributylphosphine (TBP), and nitrogen-phosphorus bonded compounds such as hexamethoxycyclotriphosphazene $((\text{N}=\text{P}(\text{OCH}_3)_2)_3)$ (HMOPA), hexamethylphosphoramide (HMPA), and N-phenyl-P,P,P-trimethylphosphorimidate (PhTMI). The inorganic compounds inhibit the reactivity of the Lewis acid PF_5 , which is the main cause of the instability of LiPF_6 .

An alternative salt such as Lithium bis(oxalato) borate (LiBOB), lithiumdifluoro oxalate borate (LiDFOB), and lithiumtetrafluoro oxalate phosphate (LTFOP) were initially studied to improve the high temperature performance of Li-ion batteries (Zhang 2006). It is shown that these kinds of alternative salt not only is capable of suppressing PC irreversible reduction, but also significantly stabilizes the SEI against the extended cycling. LiBOB can form a stable SEI containing semi-carbonate species both on the anodes and cathodes surface, as seen in Fig 2.9 (a). Oligomeric borates are also formed where the polymerization reaction is initiated through one of the two BOB anions, as shown in Fig 2.9 (b).

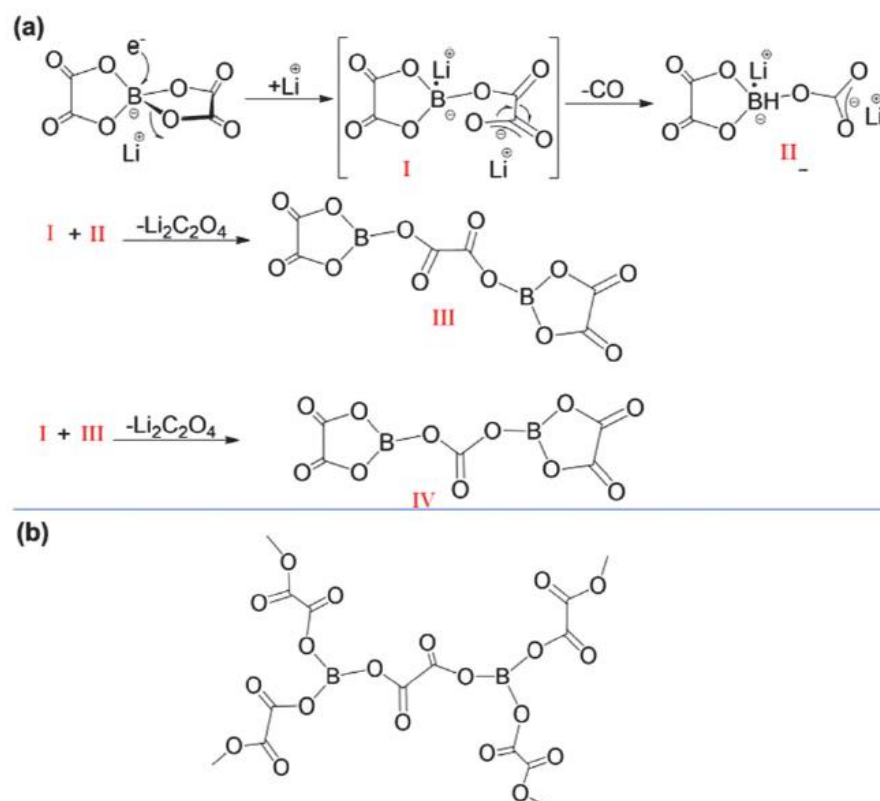


Figure 2.9: Mechanism of SEI formation by LiBOB, (a) semi-carbonate species formation, (b) oligomeric borate formation (Zhang 2006)

When the other BOB anion is electrochemically activated, there is a cross-linking reaction with various BOB-based polymer chains which leads to higher interfacial impedance. The interfacial impedance can relatively be reduced by using additives with only one oxalato group such as LiDFOB and LiTFOP. These additives form a stable SEI similar to LiBOB, however, because of the absence of the other oxalato ring, there is no cross-linking reaction which results in lower interfacial impedance than with LiBOB. Both additives improved the capacity retention and performance of a MCMB/Li^{1.1}[Ni_{1/3}Co_{1/3}Mn_{1/3}]_{0.9}O₂ cell. Moreover, the thermal stability of LiPF₆-based electrolytes can be improved in the presence of these additives by preventing the generation of PF₅ during the thermal dissociation of LiPF₆. At high temperatures, LiDFOB undergoes disproportionation reactions with LiPF₆ and forms LiBF₄ and LiPF₄C₂O₄ (Zhang 2006).

2.3.3.2 Solvent Modification

Mixed alkyl carbonates are widely used as solvent for a various lithium-ion battery applications. The most suitable solvent commonly chosen by modified or mixed with one or more other solvent to enhance their electrochemical performance. Hence, the understanding of the behavior of each solvent in the mixed system is crucial for controlling the electrolyte composition. As described in previous section, EC is the most preferred solvent in LIBs application, but it is a solid at room temperature. While PC has a problem related to the extensive solvent co-intercalation which subsequently can causes severe exfoliation of the graphite electrodes.

Atetegeb, Zhang et al. have been reported a direct comparison of the reduction of alkyl-carbonates in single, binary, and ternary solvent systems by using PC, EC/PC, EC/DEC, and EC/PC/DEC solvents for a LiPF_6 electrolyte (Haregewoin, Leggesse et al. 2014). The reduction products are identified based on Fourier transform infrared spectroscopy (FTIR) after employing linear sweep voltammetry (LSV) to certain potential regions and their possible formation mechanisms are discussed. FTIR analyses revealed that the reduction of EC and PC was not considerably influenced by the presence of other alkyl carbonates. However, DEC exhibited a different reduction product when used in EC/DEC and EC/PC/DEC solvent systems. The reduction of EC occurred before that of PC and DEC and produced a passivating surface film that prevented carbon exfoliation caused by PC.

The binary EC/DEC solvent system demonstrated most favorable performance followed by EC/PC/DEC, EC/PC, and PC electrolyte system. The DEC reduction product in the EC/DEC system contained no double bond and, consequently, no further reaction was expected during the subsequent cycles. The SEI film was expected to become stable after the first cycle, which may explain the more stable cell performance, smaller impedance, and higher Li^+ ion diffusivity of the EC/DEC system compared with other electrolyte solvent system.

2.4 Electrolyte Additives

The current state-of-the-art electrolyte systems for lithium ion batteries have their own drawbacks such as irreversible capacity, cycle-ability, temperature limits, and safety issues. One of the most economic and effective methods to minimize these problems as well as improve the electrochemical performance of LIBs is use electrolyte additive. Generally, most of electrolyte additive research focuses on forming stable and robust SEI layers. The basic idea is incorporate small concentrations of new components (additive) into the electrolyte system with the intention of changing the targeted properties of the electrolyte while maintaining its bulk properties. The role of these additives is expected to facilitate better performance of the LIBs, such as:

1. Improve the SEI layer formation, either on the anode and cathode surface.
The improvement could be the stability of the SEI layer, reduce irreversible capacity and gas generation for the SEI formation, or reduce dissolution of the electrode materials.
2. Improve physical properties of the electrolyte such as ionic conductivity, viscosity, wet-ability to the polyolefin separator, and so forth.
3. Enhance thermal stability and battery safety. These additives are expected to provide a limit protection against abuse conditions such as overcharge and elevated temperature.

Figure 2.10 show a schematic description of how surface-active additives improve the performance of graphite electrodes. The additive commonly have higher reduction potential than solvent molecules, thus it can reduce earlier to form insoluble solid products. These reduction products would be deposited and covered into graphite anode surface as preliminary protective film to de-active catalytic activity and protect the dissolution of the electrode material. The present of additive also can reduce the decomposition of the electrolyte system and increases the reversibility capacity of the battery.

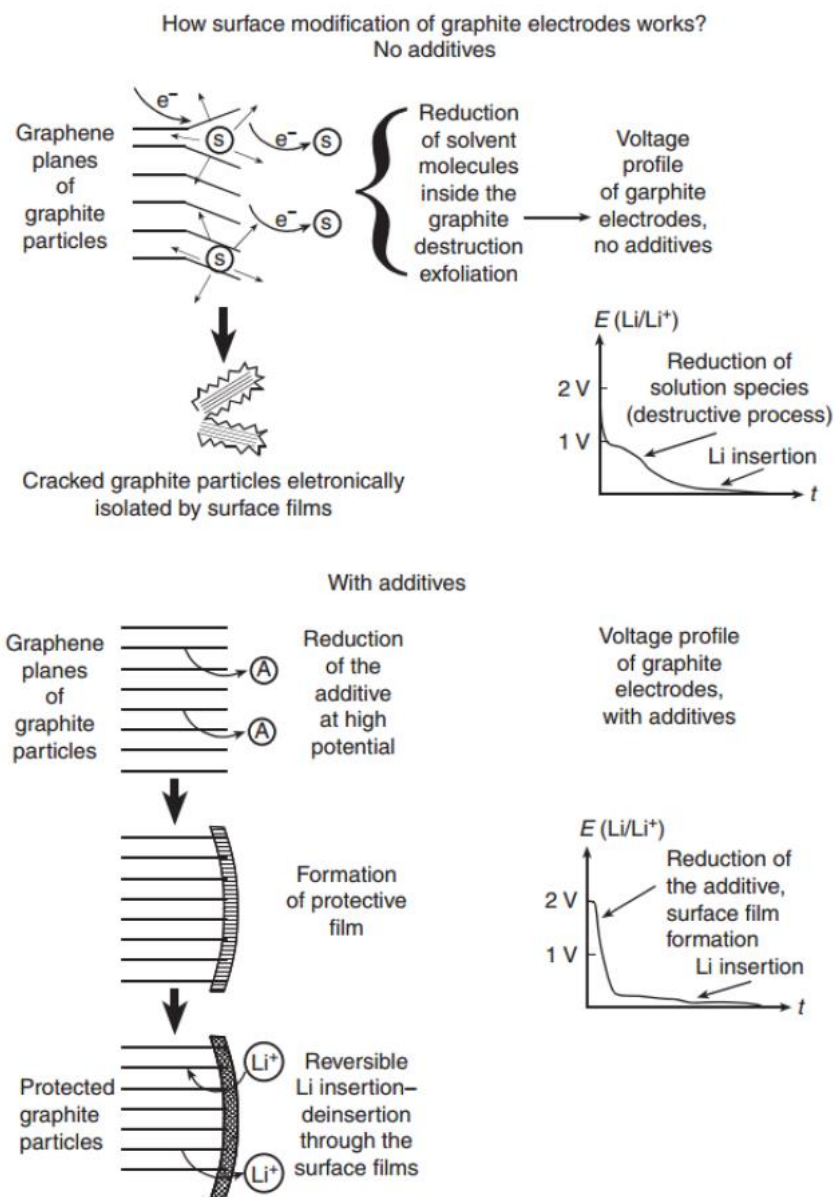


Figure 2.10: Illustration of the basic way to improve the performance of graphite electrodes by the use of electrolyte additives (Zhang, Ding et al. 2001)

In the case of graphite anode (carbon-based anode material), LIBs have some drawbacks, such as: (i) capacity fading due to the present of impurities and further decomposition of the electrolyte system, (ii) exfoliation of the graphite anode due to co-intercalation of electrolyte solvents such as PC, (iii) Degradation of the carbon anode caused by Mn dissolution when the positive electrode used spinel (LiMn_2O_4) (Zhang 2006). These problems can be overcome using SEI film forming additives which are reduced at higher potentials than the electrolyte

solvents and passivate the electrode's surface to prevent further reduction of the electrolyte solvents. The SEI film formed by the electrolyte additives is dependent on the functional group incorporated. Based on their characteristic in electrochemical processes, Zhang divided the SEI film forming additives into several categories (Zhang 2006):

a) Polymerizable monomer additives

The mechanism of the polymerizable additives in facilitating SEI formation is based on an electrochemically induced polymerization, which can be described in Fig 2.11, where the radical anion can be terminated by the solvent molecules to form an insoluble and stable product as the preliminary SEI layer. In addition to the reductive polymerization, the opposite oxidative polymerization also can occur on the positive electrode, which inevitably increases impedance and irreversibility of the cathode. Most of polymerizable additives is featured by one or more carbon-carbon double bonds in their molecules, includes vinylene carbonate (VC), vinyl ethylene carbonate, allyl ethyl carbonate, vinyl acetate, divinyl adipate, acrylic acid nitrile, 2-vinyl pyridine, maleic anhydride, methyl cin-namate, phosphonate, and vinyl-containing silane-based compounds.

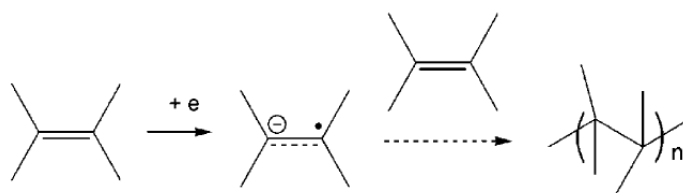


Figure 2.11: General mechanism of polymerization additives (Zhang 2006)

Vinylene carbonate (VC) is the most used electrolyte additive in LIBs application. It has been reported by SAFT that VC can reduce the decomposition of electrolyte system caused by further reaction of the alkyl carbonate solvents with their decomposition products, i.e. alkoxide anions. VC can consume the alkoxide anions and improve the electrochemical behavior, the cycling performance, and the thermal stability of LIBs systems. VC also has the ability to form a very thin polymeric film on the electrode's surface to prevent solvent decomposition and minimize the resistance of the battery.

Several authors have been reported that VC can polymerize at the surface of the negative electrode or at the positive electrode. It was suggested that VC can polymerize according to a cationic mechanism at high potential at the surface of the positive electrode, or according to an anionic mechanism at low potential at the surface of the negative electrode. The main possible degradation products of VC are depicted in Fig 2.12. It was suggested that the polymerization of VC can proceed either via the C=C double bond, leading to a polymer consisting of a repetition of EC units (polymer A), or via the carbonate group, leading after a ring opening to linear chains of polycarbonates where the C=C double bonds are maintained (polymer B). In addition, they also suggested that VC can reduce into a radical anion, which further reacts with VC to form unsaturated lithium alkyl dicarbonate salts, namely, lithium vinylene dicarbonate (LVD) ($=\text{CH}-\text{OCO}_2\text{Li}$)₂ (compound C in Fig 2.12) and lithium divinylene dicarbonate (LDVD) ($-\text{CH}=\text{CH}-\text{OCO}_2\text{Li}$)₂ (compound D in Fig 2.12), which would participate to the SEI formation. All of these degradation products would be precipitated and deposited on the electrode surface as SEI layer (Xu, Zhuang et al. 2013).

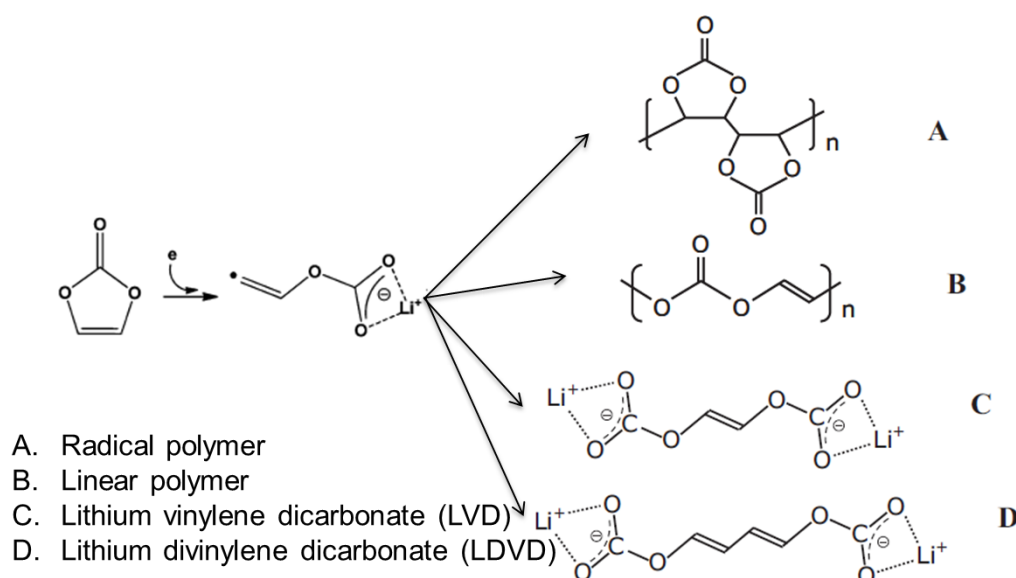


Figure 2.12: The main possible of VC degradation product (Xu, Zhuang et al. 2013)

b) Reduction agent additives

Reductive agents assist SEI formation through adsorption of their reduction products onto the catalytic active sites of graphite surface. Effectiveness of such additives in facilitating SEI formation is affected by the affinity of molecular moieties of the reduced products to the graphite active sites. Most of these kinds of additives belong to sulfur-based compounds, including SO_2 , CS_2 , polysulfide (Sx^{2-}), cyclic alkyl sulfites, such as: ethylene sulfite and propylene sulfite, and aryl sulfites.

The other reductive additives include N_2O , nitrate, nitrite, halogenated ethylene carbonate, halogenated lactone such as γ -bromo-butyrolactone, and methyl chloroformate. The later three compounds contain a carbonyl ($>\text{C}=\text{O}$) group, which can be electrochemically reduced in the similar manner as EC. Their function in facilitating SEI formation is attributed to the possible bonds between the halogen species of the SEI consisting of the reduced products of electrolyte solvents and halogen-containing additive.

Fluoroethylene carbonate (FEC) is the most commonly used additive for both Si and Sn based electrodes. FEC usually used as a co-solvent in Si based electrodes. When the Si anode is cycled with a FEC free electrolyte, a less dense SEI containing $-\text{Si}-\text{C}$ and $-\text{Si}-\text{O}$ functional groups is formed. Since $-\text{Si}-\text{C}$ and $-\text{Si}-\text{O}$ bonding is not too strong, thus further decomposition of the electrolyte system occurs during cycling which leads to continuous SEI formation. The addition of low concentration of FEC as a co-solvent can suppress the continuous SEI formation by forming $-\text{Si}-\text{F}$ and LiF species which have strong bonding energy. FEC is an interesting compound, which itself does not contain vinyl group. However, FEC can forms polymeric species by generating HF to form VC and polymerizes through the double bond as shown in Figure 2.13. FEC has a great influence on the cycling performance of the battery when 5% FEC was used. However, when the amount of FEC was increased, the formation of LiF increased by consuming lithium ions leading to a higher irreversible capacity.

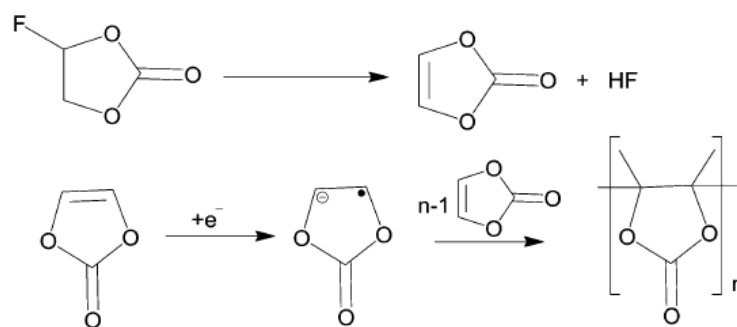


Figure 2.13: Reduction reaction mechanism of FEC which lead to the formation of polymeric species (Haregewoin, Wotango et al. 2016)

c) Reaction type additives

In fact, this type of additives may not be reduced electrochemically in the whole potential range of lithium ion intercalation. However, they are able to form more stable SEI components by reaction with an intermediate compound of the solvent reduction or combine with the final products such as lithium alkyl dicarbonate and lithium alkyl oxide. In addition, the present of CO_2 in this type of additives can facilitate the SEI formation, reduced the initial irreversible capacity and stabilized SEI as seen in Figure 2.14. These kinds of reaction mechanism commonly belong to a series of carboxyl phenol, aromatic esters, maleic anhydride, succinimide and N-benzyloxy carbonyloxy succinimide. All these additives are believed very effective in suppressing PC reduction and stabilizing the SEI formation. In some cases, such additives may not reduce the irreversible capacity of the first cycle, but significantly increase the cycle-ability of the LIBs.

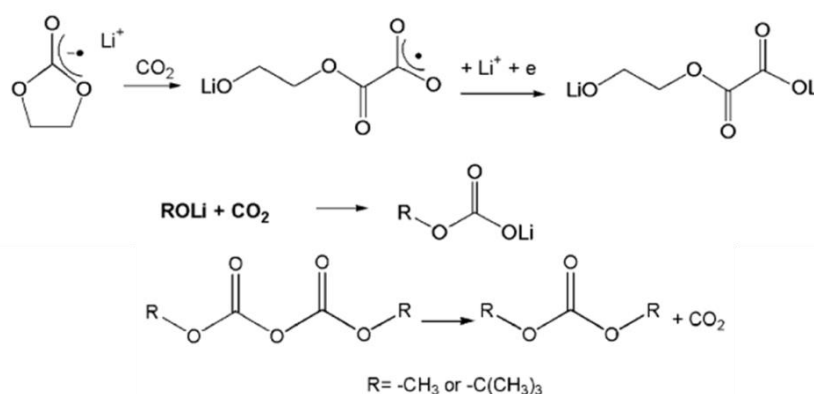
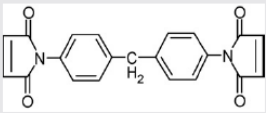
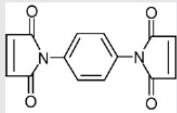
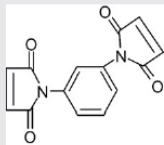


Figure 2.14: Reaction mechanism of reaction type additives (Zhang 2006)

2.5 Maleimide-based Additive

Recent progress of electrolyte additive is developing a new maleimide-based additive. Maleimide (MI) additives, which are polymeric film forming agents, capable to enhance the rate capability and cycle-ability due to its high LUMO energy, high reductive potential and unique reaction mechanism compared with alkyl carbonate, such as EC, PC, and DEC. Wang et al. elucidated three maleimide (MI)-based aromatic molecules as additives in electrolyte that is used in lithium ion batteries (Wang, Cheng et al. 2009).

Table 2.8: The chemical structures of MI-based additives and the oxidation potentials measured from HOMO, LUMO orbital energies

Compounds			
	MI-1	MI-2	MI-3
			
HOMO (eV), S	-6.19	-5.79	-6.47
LUMO (eV), S*	-5.80	-6.43	-6.57
Oxidation potential (V) vs. Li/Li*	4.54	4.65	5.06

Source: (Wang, Cheng et al. 2009)

Table 2.8 presents three maleimide (MI)-based electrolyte additive with orbital energy of the molecules' HOMO, and the cation's LUMO in the solution. Based upon molecular orbital theory, a molecule with a lower energy level of lowest unoccupied molecular orbital (LUMO) should be a better electron acceptor and more reactive on the negatively charged surface of the electrode (Xu, Zhuang et al. 2013). All of the MI-based additives have lower LUMO energies (Table 2.8) than the alkyl carbonates, such as EC, PC and DEC reaction (Whittingham 2004, Haregewoin, Leggesse et al. 2014). Therefore, the MI-based additives have higher reduction potential, preventing a competitive reaction between MI and the alkyl carbonates. Electrolyte additives that have a higher reduction potential typically are associated with better battery performance. This study proven that the MI-based additives can prompt the formation of a solid electrolyte interphase (SEI); and inhibit the entering into the irreversible state during lithium intercalation and co-intercalation. The MI is used in lithium ion batteries and provided 4.9% capacity increase and 16.7% capacity retention increase when cycled at 1C/1C.

The MI-based additive also ensures respectable cycle-ability of lithium ion batteries.

Based on the structure, MI-2 and MI-3 each have a phenyl group in the middle of the structure, providing very high electrochemical stability because the Π (phi) orbital is conjugated and because of the resonance structure of the phenyl group. Although MI-1 has two phenyl groups on each of its two sides—they do not improve electrochemical stability, because MI-1 has a methyl group in the middle of its structure, which pushes an electron out of the structure, potentially breaking it down, such that the MI-1 has a lower oxidation potential than the two other additives.

Wang et al. also reported a series of phenylenedimaleimide compounds having the maleimide group in the ortho (i), para (ii), and meta (iii) positions (Fig 2.15). They reported that all of the MI additives were reduced prior to the solvents to form a stable SEI on the electrode's surface, while showing a better performance than the additive free electrolyte. However, the additives with the para position substituents showed a better performance than those with ortho and meta position substituents. Although their reduction mechanism is similar, they show various SEI film distributions and densities. The additive at the para position forms a dense and highly uniform SEI. However, the ortho position shows loose and discontinuous SEI formation (Cheng, Wang et al. 2012).

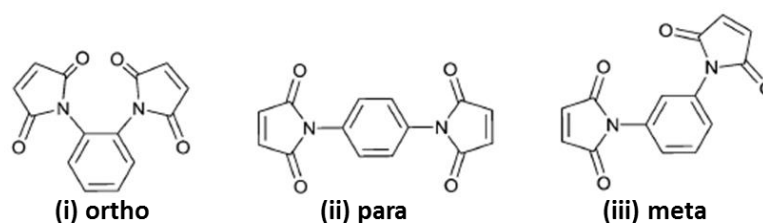


Figure 2.15: Chemical structure of phenylenedimaleimide positional isomers (Haregewoin, Wotango et al. 2016)

In addition, Wang et al. also develop a novel binary additive by combine MI-based additive as a primary additive and H_2O as secondary. This method is a viable strategy to increase both the charge/discharge rate and cycling ability of LIBs. Although, the MI/ H_2O binary additive displays a remarkable combination of high rate and high capacity at high temperatures; however, several factors, such as

thermal stability, overcharging issue, and the extra cost of the MI additive, must be considered before considering its application in commercial products. If the outcome of such development studies is positive, MI/H₂O would be the optimal potential electrolyte additive for lithium ion battery applications (Cheng, Wang et al. 2012).

2.6 The Electronegativity Functional Group Effect on Electrolyte Additive

Wang et al. argued that a major issue in SEI formation on the anode's surface is that the additive needs to have strong electron-withdrawing groups with a high reduction potential (Wang, Cheng et al. 2009, Wang, Yu et al. 2013). Additives containing high electronegativity and high electron withdrawing functional groups such as –CN, Cl, and F can make the compound more electrophilic and facilitate the reduction reaction mechanism (Haregewoin, Wotango et al. 2016). If the additive contains a vinyl group, reduction of the additive may lead to the formation of an SEI with a polymeric structure in which polymerization is initiated by the vinyl group.

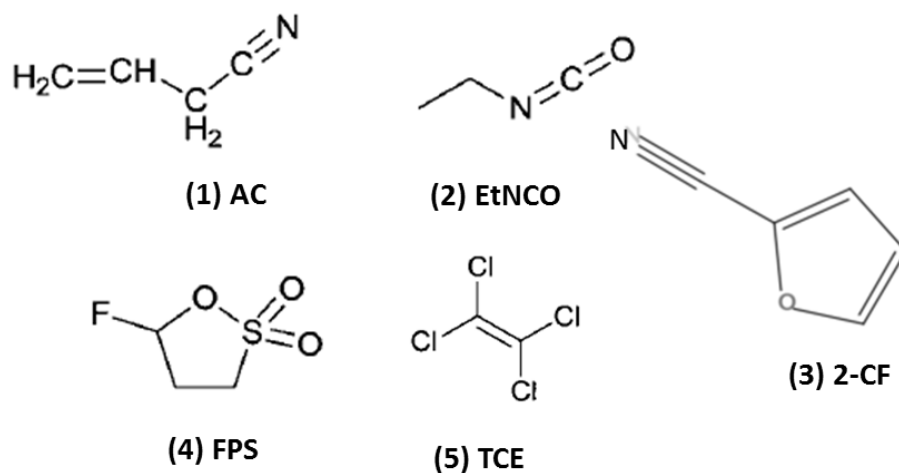


Figure 2.16: Chemical structure of additives containing electronegativity and electron withdrawing functional groups (Haregewoin, Wotango et al. 2016)

Yong et al. showed that low concentration of allyl cyanide (AC, **1**) allows the use of a PC based electrolyte for the graphite electrode by forming a polymeric SEI on the electrode's surface. The polymerization is initiated by the

double bond of AC, followed by a chain reaction. Similarly, in acrylic acid nitrile (AAN), which contains a mixture of vinyl groups and electron-withdrawing groups, the electro-polymerization reaction is initiated by radical anions formed by the reduction of vinyl groups (Chai, Wen et al. 2011). When ethyl isocyanate (EtNCO, **2**) is used as an additive, its reduction leads to the formation of a polymeric film which is initiated by the reaction of the isocyanate group (Santner, Möller et al. 2003). 2-cyanofuran (2CF, **3**) is a new vinylene group containing additive for propylene carbonate-based electrolytes shows good SEI-forming behavior on graphite and suppresses solvent co-intercalation (Korepp, Santner et al. 2006). The reduction processes is initiated by reaction of the double bond of the vinylene compound and it is an important step of the SEI formation process.

3-fluoro-1,3-propane sultone (FPS, **4**), which is a modification of PS made by introducing an electron withdrawing fluorine group, showed better performance compared with PS and VC in a LiCoO_2 /graphite cell (Jung, Park et al. 2013). The presence of the fluorine group enhances the anodic stability and cathodic reactivity of the additive which helps to improve its SEI forming ability. In addition, Tetrachloroethylene (TCE, **5**) is another electrolyte additive reported by Hu et al. for PC based electrolytes (Hu, Kong et al. 2005). TCE show that 3% of the additive can suppress the co-intercalation of PC and the decomposition products of TCE form an effective SEI on the graphite anode and lead to the improving cell performance. Moreover, TCE also allow the use of 4 V cathodes since the oxidation potential of the electrolyte is as high as 4.5 V vs. Li/Li^+ .

“This page intentionally left blank”

CHAPTER III

RESEARCH METHODOLOGY

3.1 Research Design

The electronegativity functional group effect of the fluoro (F) and cyano (CN) functional group on the maleimide-based additive in lithium ion battery is first started by preliminary experiment of the electrode and electrolyte preparation. Commercial MCMB is used as anode material, the lithium foil is used as cathode material for half-cell system, and LiCoO_2 is used as cathode material on full cell system. Commercial electrolyte 1 M lithium hexafluorophosphate (LiPF_6) in ethylene carbonate (EC): propylene carbonate (PC): di-ethylene carbonate (DEC) (3:2:5 in volume) was used as blank electrolyte system and 0.1 wt% maleimide-based additives were dissolved and mixed into the electrolyte. These additives were 4-fluoro-phenylenedimaleimide (F-MI), 4-cyano-phenylenedimaleimide (CN-MI), and commercial additive o-phenylenedimaleimide (O-MI) as comparison.

The electrochemical performance analysis would be based to determine the reduction potential of the maleimide-based additives, the effect of the additive presence and the electronegativity functional group effect on maleimide-based additives. These tests could also observe the cell behavior, especially the capacity retention and rate capability. CV is used to determine the electrochemical performance and EIS test for the evaluation of system resistance after several cycles. Finally, in order to investigate the role of this additive and its effects to the battery performance, several surface characterization and analysis, such as: SEM and EDX were performed.

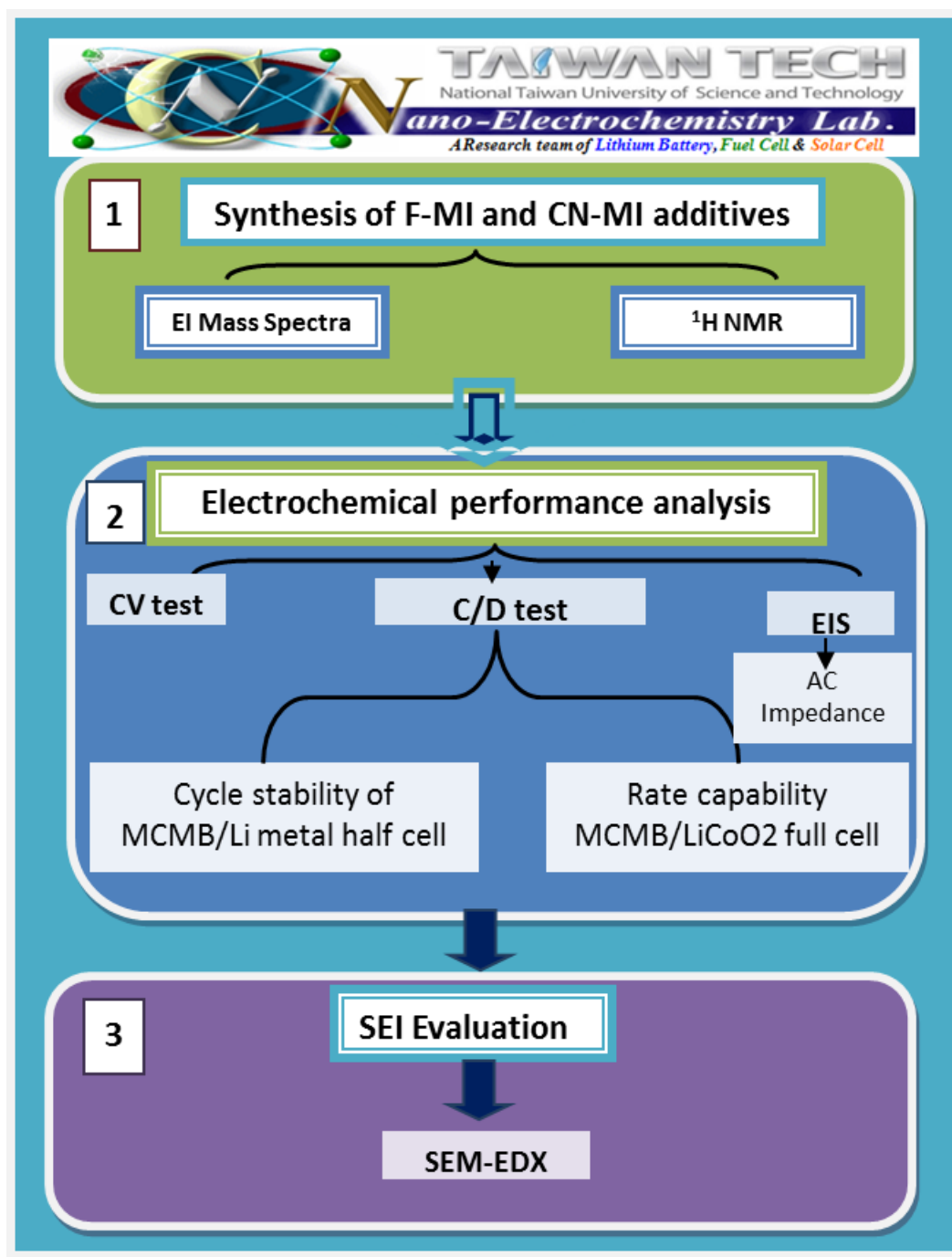


Figure 3.1: Flow chart of research design

3.2 Materials

The materials were used in this experiment includes:

1. 4-fluoro-nitroaniline, diamino-benzonitrile
2. 4-fluoro-phenylenedimaleimide (F-MI), 4-cyano-phenylenedimaleimide (CN-MI), and o-phenylenedimaleimide (O-MI) (Aldrich, 98%)
3. 1 M lithium hexafluorophosphate (LiPF_6) in ethylene carbonate ($\text{C}_3\text{H}_4\text{O}_3$): propylene carbonate ($\text{C}_4\text{H}_6\text{O}_3$) :diethyl carbonate ($\text{C}_4\text{H}_6\text{O}_3$) 3:2:5 v/v
4. 3% hydrogen in argon gas
5. Ethanol 95 % ($\text{C}_2\text{H}_6\text{O}$)
6. Acetone 95% ($\text{C}_3\text{H}_6\text{O}$)
7. Hydrazine hydrate 98 % (N_2H_4)
8. Palladium activated carbon, 10% loading
9. Maleic anhydride 99% ($\text{C}_4\text{H}_2\text{O}_3$)
10. Triethylamine 99.5 % (C_2H_5)₃N)
11. Magnesium chloride hexahydrate 99% (MgCl_2)
12. Acetic anhydride 99 % ($(\text{CH}_3\text{CO})_2\text{O}$)
13. DI water (H_2O)
14. Positive electrode (cathode)

The cathode material consisted of 91 wt% lithium cobalt oxide (LiCoO_2 -LICO Corp., Taiwan) as the active material, 5 wt% of KS-6, and 4 wt% PVDF.

15. Negative Electrode (anode)

The anode material consisted of 93 wt% mesocarbon microbeads (MCMB-2528, Osaka Gas), 3 wt% KS-6 as a conductive additive (KS- 6, Showa, Japan), and 4 wt% PVDF as a binder (Kureha Chemical, Japan).

16. Electrolytes

This study was used 4 types of electrolytes:

- Blank : 1 M LiPF_6 EC:PC:DEC 3:2:5 v/v
- O-MI : 1 M LiPF_6 EC:PC:DEC 3:2:5 v/v , 0.1 % wt O-MI
- F-MI : 1 M LiPF_6 EC:PC:DEC 3:2:5 v/v , 0.1 % wt F-MI
- CN-MI : 1 M LiPF_6 EC:PC:DEC 3:2:5 v/v , 0.1 % wt CN-MI

3.3 Equipments

Some equipments were used during the experiments process, such as:

1. Argon gas Glove, MEMMERT
2. Battery cycler
3. Cyclic Voltammeter (CV) and Electrochemical Impedance spectroscopy (EIS), Biologic EC-Lab
4. Digital analytical balance
5. Field-Emmision Scanning Electron Microscope, JEOL JSM-6500F
6. Hot plate and stirrer
7. Vacuum oven
8. EI mass spectrometer
9. Nuclear magnetic resonance, Varian Germini 200

3.4 Experimental Procedure

3.4.1 Synthesis of F-MI and CN-MI additive

The Additives used in this study is developing from the malemaide-based additives by attaching element with a high electron withdrawing group and a high electronegativity (fluorine and cyanide). The additives, 4-fluoro-o-phenylenedimaleimide (F-MI) and 4-cyano-o-phenylenedimaleimide (CN-MI) were prepared by a one pot synthesis developed by Orphanides et al. F-MI additive was synthesized using two parts of methods: hydrogenation and dehydration (Fig 3.2). Meanwhile, CN-MI additive only was synthesized by dehydration method (Fig 3.3). The synthesis results were characterized using el mass spectrometry and nuclear magnetic resonance (NMR) spectroscopy.

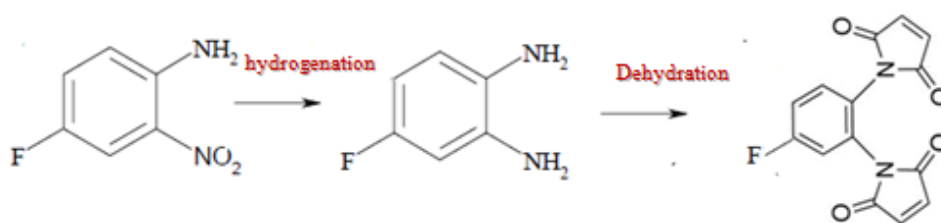


Figure 3.2: F-MI synthesis mechanism

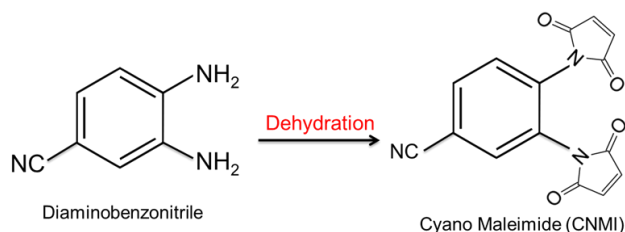


Figure 3.3: CN-MI synthesis mechanism

Hydrogenation Part

The procedure of synthesis the 4-flouro-phenylenediamine is explained below: a glass flask (with feeding pipe) equipped with a thermometer, mechanical paddle stirrer and a water cooled condenser. A solution of 4-flouro-nitroaniline (10 gr), palladium activated carbon (0.5 gr) (10% loading), ethanol (59.61 ml) is added into the glass, hydrazine hydrate (7.983 ml) is added to the feeding pipe. The heterogeneous reaction mixture is maintained until the temperature reach

80°C. When the temperature was raised to 80 °C, hydrazine hydrate is added into the glass by open the feeding pipe gradually, the hydrogenation process was occurred, and the reaction mixture is maintained up to 24 hours. The precipitated product is cooled by vacuum filtration, washed with ethanol, and dried for 24 hours at 60 °C in vacuum oven. Figure 3.4 shows the reaction mechanism of hydrogenation processes.

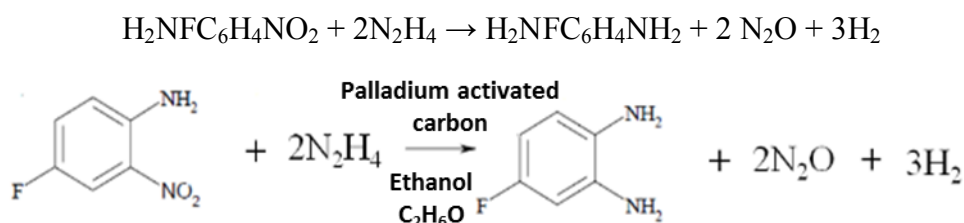


Figure 3.4: Reaction mechanism of hydrogenation part

Dehydration Part

A flask is with a thermometer, mechanical paddle stirrer and a water cooled condenser. To a solution of maleic anhydride (1.92 parts) in 4.8 parts acetone is added a solution of 1 part precursor (4-flouro-phenylenediamine for F-MI additive or diamino-benzonitrile for CN-MI additive), 0.32 parts triethylamine and 1.6 parts acetone over a 15-minute period. A precipitate formed during that time. The heterogeneous reaction mixture is maintained at 40°C, for 30 minutes. Magnesium chloride hexahydrate (0.08 parts) and 2.44 parts acetic anhydride were added all at once. The temperature is raised to 50 °C and maintained for 3 hours. After 30 minutes, the reaction mixture became homogeneous and amber in color. Five minutes later, the products begin to precipitate. At the end of the reaction time, the mixture was cooled and 12 parts water added. The precipitated product is cooled by vacuum filtration, washed with ethanol, and dried for 24 hours at 60 °C in vacuum oven. The yield results were characterized by mass spectral and Nuclear Magnetic Resonance (NMR) analysis. Figure 4.4 shows the reaction mechanism of dehydration processes. Maleic anhydride is reacted with the precursor 4-flouro-o-phenylenediamine and opens the amine ring and become the 4-flouro-o-bismalemaicacid as shown in Fig. 3.5, then after dehydration process by triethylamine. The ring is closed and become the maleimide.

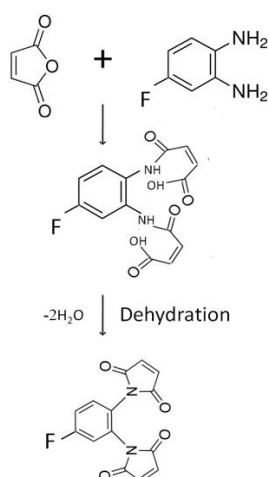


Figure 3.5: Reaction mechanism of dehydration part

3.4.2 Electrolyte Preparation

This study was used 4 types of electrolyte preparations.

Blank electrolyte

The blank electrolyte is lithium hexafluorophosphate (1 M) which is dissolved into ethyl carbonates (EC): propyl carbonate (PC): diethyl carbonate (DEC) (3:2:5 by volume) mixed solvents.

O-MI additive-based electrolyte

The lithium hexafluorophosphate (1 M) is dissolved into EC:PC:DEC (3:2:5 by volume) mixed solvents. O-MI (0.1 wt%), is then completely dissolved in the multi-carbonate-based liquid electrolyte at room temperature, and is used as the primary organic, small molecular weight additive.

F-MI additive-based electrolyte

The lithium hexafluorophosphate (1 M) is dissolved into EC:PC:DEC (3:2:5 by volume) mixed solvents. F-MI (0.1 wt%), is then completely dissolved in the multi-carbonate-based liquid electrolyte at room temperature, and is used as the primary organic, small molecular weight additive.

CN-MI additive-based electrolyte

The lithium hexafluorophosphate (1 M) which is dissolved into EC:PC:DEC (3:2:5 by volume) mixed solvents CN-MI (0.1 wt%), is then completely dissolved in the multi-carbonate-based liquid electrolyte at room temperature, and is used as the primary organic, small molecular weight additive.

3.4.3 Electrochemical Measurement

The electrochemical performance analysis was used in this study were conducted by cyclic voltammetry (CV), electrochemical impedance spectroscopy (EIS), and charge/discharge measurement.

Battery Coin Cell Assembling

The 2032-type coin cell is being used on this work. The coin cell is assembled using MCMB electrode as the anode and the lithium metal as cathode for half-cell and LiCoO_2 electrode as cathode for full cell. Meanwhile, 0.1 % amount of additives was dissolved into the 3:2:5 by volume of EC, PC and DEC with 1.1M LiPF_6 salt of electrolyte. Polypropylene membrane is used as a membrane separator. All of processes for the battery fabrication and electrolyte preparation were performed inside an argon-filled glove box in order to avoid interference from moisture effect. The arrangement of the coin cells in depicted in Fig 3.6. The coin cells were tested using the programmable battery tester in the potential range 0 to 3 V for MCMB/Li anode half-cell at room temperature and 3 to 4.2 V for MCMB/ LiCoO_2 full cell at room temperature.

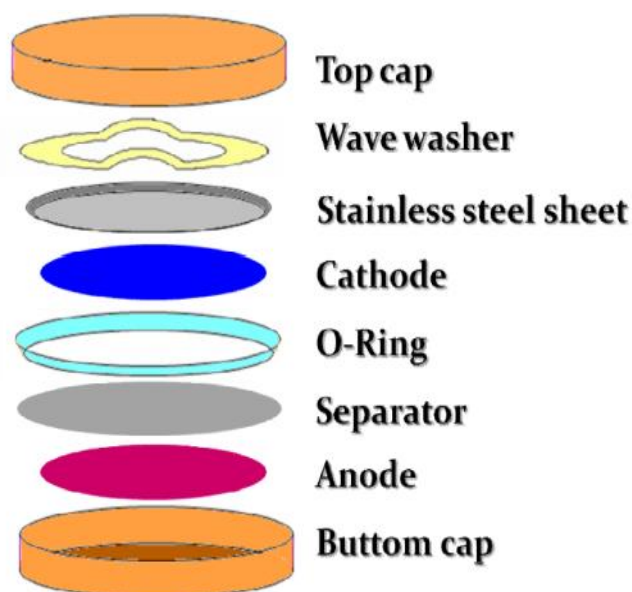


Figure 3.6: Schematic Arrangement of Coin Cell Assembly

Cyclic Voltammetry measurement

The electrochemical stability of electrolytes is measured by cyclic voltammetry (CV) using a Biologic VMP3 from -0.1 to 3 V at a scan rate of 0.1 mV.s⁻¹ with a three-electrodes system, consisting of stainless steel working and counter electrodes with an area of 1.0 cm² and lithium reference electrodes, and also from 0 to 3 V at a scanning rate of 0.1 mV.s⁻¹ was made with an anode half-cell (CR2032) consisting of MCMB working, lithium metal counter electrodes (area 1.0 cm²). The electrolytes filled the space between the working and the counter electrodes.

Electrochemical Impedance Spectroscopy Test

Electrochemical impedance spectroscopy (EIS) is performed using a Biologic VMP3 in the frequency range 1 M to 0.01 Hz with AC amplitude of 10 mV at 25 °C. All EIS measurements employed a half cell (CR2032) consisting of MCMB electrodes (area 1.0 cm²) and lithium metal. The electrolytes filled the space between the MCMB electrode and lithium metal. Riveted refinement of the equivalent circuit model is used to simulate and demonstrate the physical meanings of the semicircles in the EIS spectra. R1 is defined as the electrolyte resistance, R2 is the bulk resistance of the SEI, and R3 is the contact resistance between the SEI and the electrode's surface.

3.4.4 SEI Evaluation Measurement

Scanning Electron Microscopy

The morphology of the electrode surface regarding the SEI layer for MCMB without and with MI-based additives is investigated by scanning electron microscopy (SEM) JEOL JSM- 6500F using 15keV of energy with different magnification up to 5000 times enlargement. The purpose is to observe the SEI morphology, particularly after additive addition into the electrolyte. In addition, Energy Dispersive X-Ray Spectroscopy (EDX) analysis is also performed in order to do elemental analyses of the SEI layer.

“This page intentionally left blank”

CHAPTER IV

RESULT AND DISCUSSION

4.1 Characterization of New Additives

As described before that the synthesis results were characterized using el mass spectrometry and nuclear magnetic resonance (NMR) spectroscopy.

4.1.1 Mass spectral of 4-fluoro-phenylenediamaleimide (F-MI)

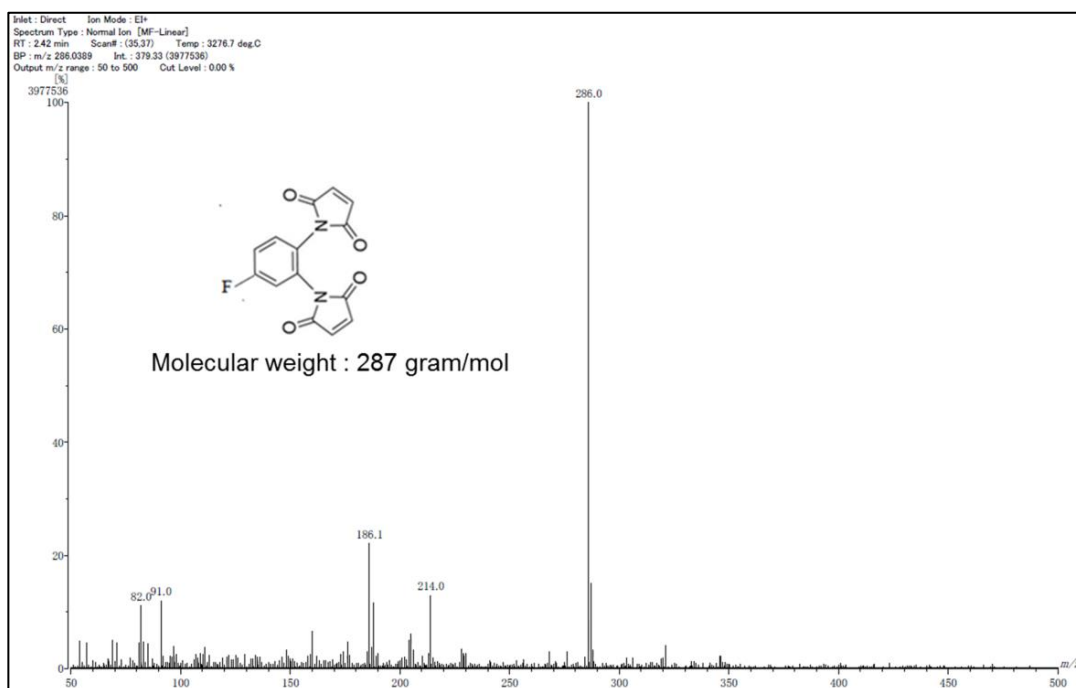


Figure 4.1: Mass spectral of F-MI

The result of mass spectral is verified by molecular weight of F-MI. Figure 4.1 shows the highest peak intensity was at 286 and the molecular weight of F-MI is 287 gram/mol. This peak shift is suspected due to the resonance of the mass spectral measurement. This result will be in line with the NMR result to check the yield of F-MI

4.1.2 ^1H NMR of 4-fluorophenylenediamaleimide (F-MI)

The ^1H NMR of F-MI is verified by ^1H NMR of commercial N,N'-o-phenylenediamaleimide (O-MI).

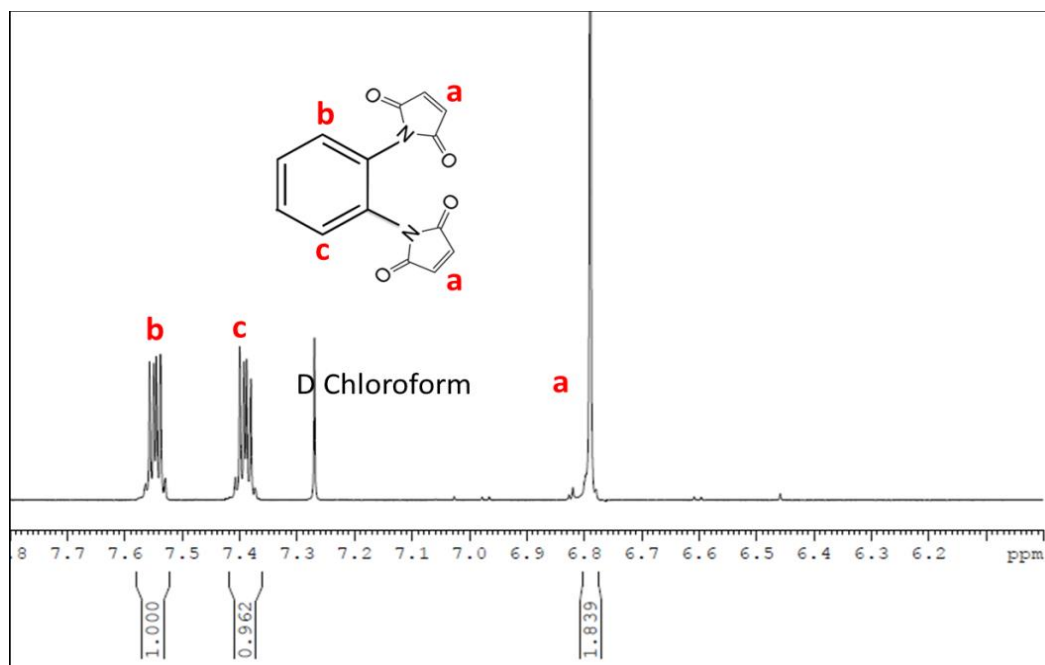


Figure 4.2: ^1H NMR of N,N'-o-phenylenediamaleimide (O-MI)

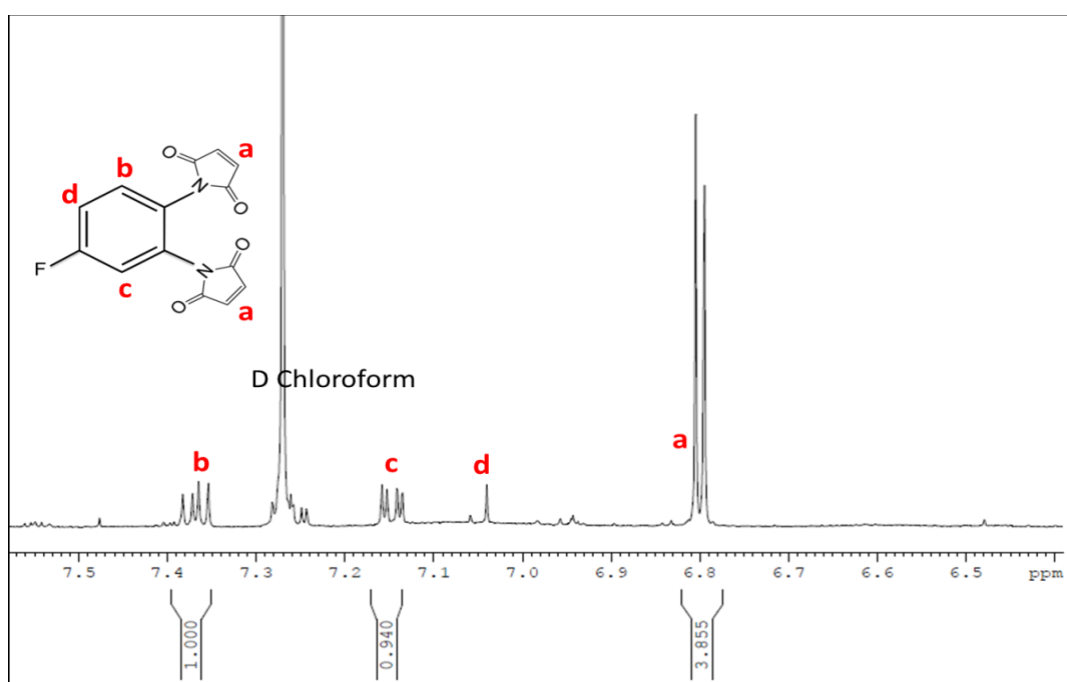


Figure 4.3: ^1H NMR of 4-fluorophenylenediamaleimide (F-MI)

Figure 4.3 is ^1H NMR of F-MI, the predicted peaks are peak a, b, c and d as verified by ^1H NMR of commercial O-MI (Fig 4.2). Peak a observed at 6.805 ppm and 6.795 ppm is peak of the proton at the two of maleimide compounds. Peak b observed at 7.354-7.382 ppm, peak c observed at 7.136-7.158 ppm, and peak d observed at 7.040 are peak of the proton at the benzene ring. Corresponded to the ^1H NMR of commercial O-MI, the addition of fluorine (F) functional group on the MI-based compound causes shifting of the proton peak at the benzene ring. In addition, it also was found a new peak at ^1H NMR of F-MI (peak d), where it was not found on the ^1H NMR of commercial O-MI due to the symmetry of the benzene ring.

4.1.3 Mass spectral 4-cyano-phenylenediamaleimide (CN-MI)

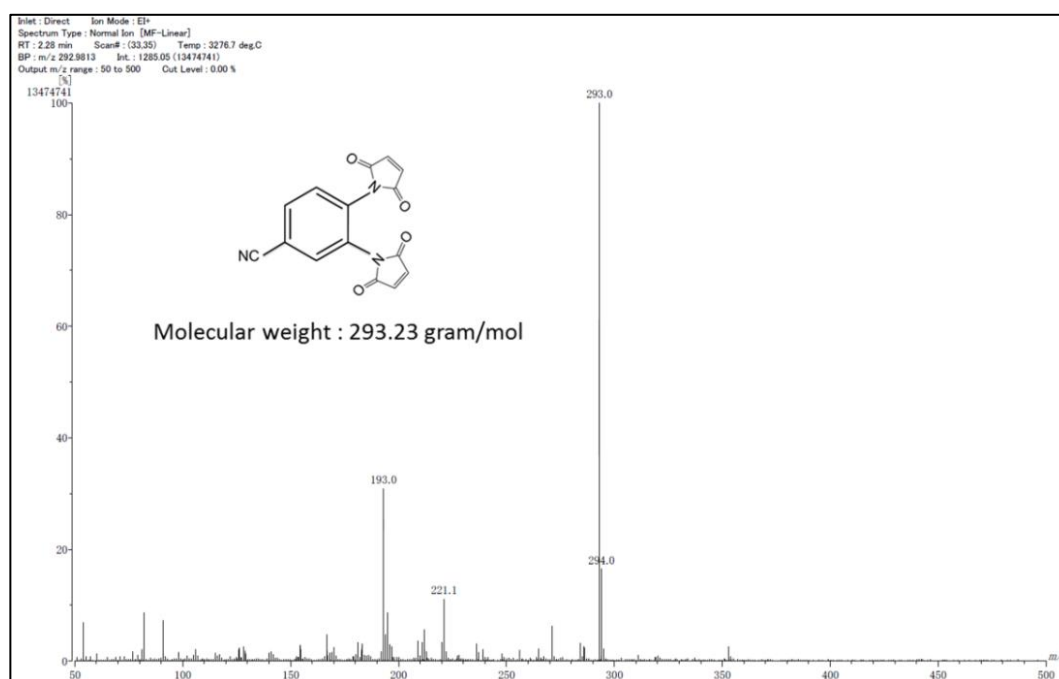


Figure 4.4: Mass spectral of CN-MI

The result of mass spectral is verified by molecular weight of CN-MI. As Fig 4.4, it can be seen that the peak observed at 293.0 is the peak of CN-MI, as verified by the molecular weight of CN-MI, which is 293.23 gram/mol. From this result, we can conclude that the CN-MI additive has successfully synthesized.

4.1.4 ^1H NMR of 4-cyano-phenylenediamaleimide (CN-MI)

The ^1H NMR of CN-MI also was verified by ^1H NMR of commercial N,N'-o-phenylenedimaleimide (O-MI).

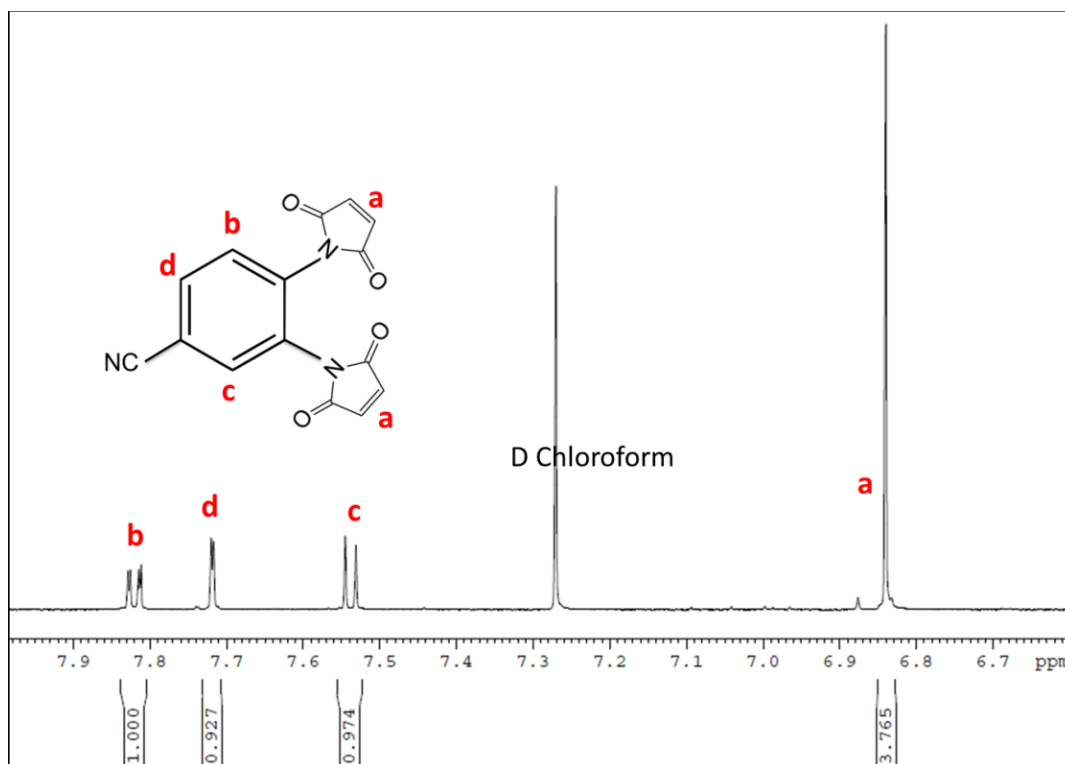


Figure 4.5: ^1H NMR of cyano-phenylenediamaleimide (CN-MI)

Figure 4.5 is ^1H NMR of cyano-phenylenediamaleimide (CN-MI) the predicted peaks are peak a, b, c and d also as verified by ^1H NMR of commercial O-MI (Fig 4.2). Similar with ^1H NMR of F-MI, peak a observed at 6.840 is peak of the proton at the two of maleimide compounds. Peak b observed at 7.812-7.829 ppm, peak c observed at 7.531-7.545 ppm, and peak d observed at 7.717-7.720 ppm are peak of the proton at the benzene ring. Corresponded to the ^1H NMR of commercial O-MI, the peak of the proton observed at the benzene ring has shifted to the left due to the cyano (CN) functional group attached on the MI-based compound and the peak d is not observed on the ^1H NMR of commercial O-MI due to the symmetry of the benzene ring.

4.2 Electrochemical Analysis

Electrochemical instruments tested in this study are cyclic voltammetry (CV), electrochemical impedance spectroscopy (EIS), and charge and discharge measurement.

4.2.1 Cyclic Voltammetry (CV) Test

Anode half-cell was assembled for each electrolyte with MCMB as anode and lithium foil as a cathode. Figure 4.6 depicts a plot of typical cyclic voltammetric curves for 4 types electrolyte of anode half-cell with range potential -0.1 to 3 V (versus Li/Li⁺). From the CV curves (Fig 4.6) show that the electrolyte with additives (O-MI, F-MI, and CN-MI) reveal an interesting electrochemical behavior compared to the blank electrolyte (without any additive). Table 4.1 shows the value of the reduction potential peak which also can be determined as electrolyte decomposition. Based upon molecular orbital theory, a molecule with a lower energy level of lowest unoccupied molecular orbital (LUMO) should be a better electron acceptor and more reactive on the negatively charged surface of the electrode (Xu, Zhuang et al. 2013). In the EC/PC/DEC system, based on the DFT calculation and experimental measured (Wang, Cheng et al. 2009, Haregewoin, Leggesse et al. 2014), the sequence of the energy level of LUMO MI-based additives (F-MI, CN-MI, and O-MI) are lower than EC, PC, DEC solvent. In other words, MI-based additives will be decomposed earlier at highest voltage followed by decomposition of EC, then PC and lastly the DEC solvent during the first lithium ion insertion process.

According to the enlarged picture in Fig 4.6 and Table 4.1, the three of MI-based additives show similar peak reduction potential and current density response that locates at high voltage (2.35 - 2.32 V). It indicates that the reduction reaction mechanism processes for O-MI, F-MI, and CN-MI additives is almost the same. The phenomena of the higher reduction potential indicated that the MI-based additive can reduce earlier, suppress the decomposition of the electrolyte, and also prevent the further reaction between electrode and electrolyte system. In contrary, no peak can be observed at the high potential from the blank electrolyte, indicating that the solvent will decompose at first time. In other words, the

formation of the SEI layers on electrolyte containing MI-based additives much faster than the blank electrolyte. Furthermore, by attaching molecule with high electronegativity and high electron withdrawing group (F and CN) also slightly affect to the MI-based additives and solvent reduction reaction mechanism. F-MI additive has highest reduction potential peak at 2.35 V, followed by CN-MI at 2.34 V, and O-MI at 2.32 V. It is believed that stronger electron withdrawing substitution (F and CN) may attract electrons on lower LUMO, which decreases the energy band gap to early reduce on anode surface. In addition, the cells containing MI-based additives also provide higher reversibility capacity when they compared with the blank electrolyte. CN-MI additive has highest reversibility capacity (47.34%), followed by F-MI (46.54%), O-MI (43.86), and blank electrolyte (40.08%). Thus, we can conclude that the cells containing MI-based additives (O-MI, F-MI, and CN-MI) can provide higher electrochemical stability and higher reversibility capability compares with the blank electrolyte.

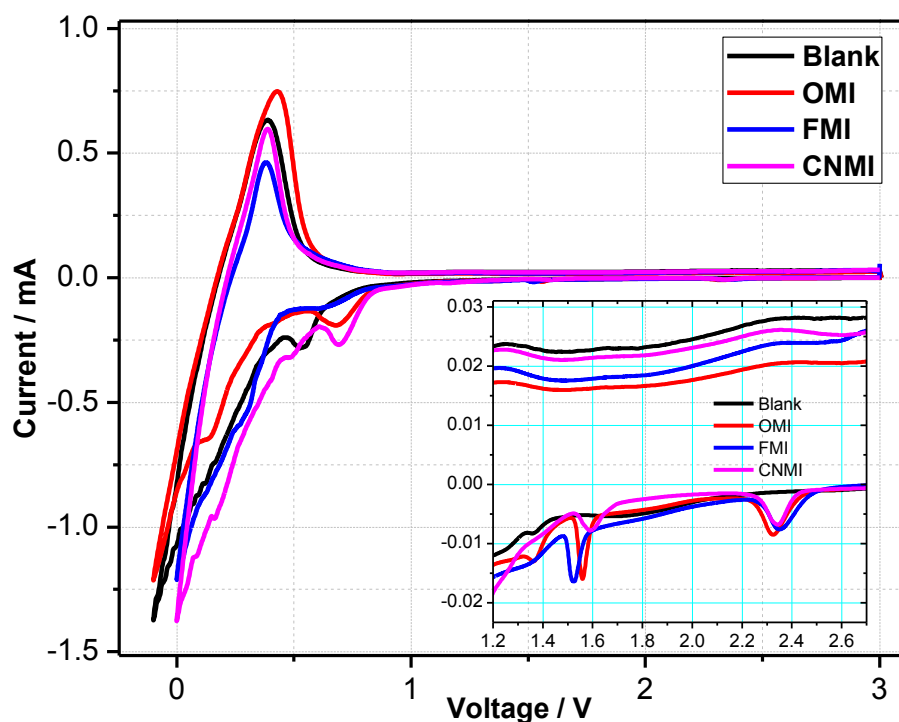


Figure 4.6: Cyclic voltammograms of lithium plating/stripping on the anode half-cell with different electrolyte. Anode half-cell with MCMB as anode and lithium foil as cathode, scan rate 0.2 mV/s and cut off voltage -0.1 – 3V vs Li/Li⁺.

Table 4.1: Reduction potential peak of MCMB/Li⁺ anode half-cell

Decomposition of electrolyte system	Blank	O-MI	F-MI	CN-MI
MI-based additive	-	2.32 V	2.35 V	2.34 V
EC	1.70 V	1.56 V	1.52 V	1.59 V
PC	1.36 V	1.36 V	1.36 V	1.16 V
DEC	0.53 V	0.68 V	0.62 V	0.69 V
Reversibility (%)	40.08	43.86	46.54	47.34

4.2.2 Charge Discharge Test

4.2.2.1 Charge Discharge Profile on MCMB/Li half cell

Figure 4.7 shows the battery performance obtained by analyzing the significance of electronegativity functional group effects in MCMB/Li⁺ half-cell. From the inset **(I)** in Fig 4.7 **(a)**, it shows that the electrolyte with the CN-MI additive possesses the highest discharge capacity (328.4 mAh/g) at the first cycle, followed by electrolyte with F-MI additive (324.6 mAh/g), electrolyte with O-MI additive (322.5 mAh/g), and the blank electrolyte (313.4 mAh/g), respectively. This phenomenon is suggested by high energy density of the electrolyte with MI-based additives, similar to the same evidence from CV result. In addition, from inset **(III)** in Fig 4.7 **(a)**, it can be seen that the slowly decreasing potential occurred at the battery with electrolyte containing F-MI and CN-MI additive. In contrast, the battery with electrolyte containing O-MI additive and blank electrolyte shows clearly sloping line which occurred at 0.6 V (low potential). Moreover, from the inset **(II)** in Fig 4.7 **(a)**, it shown that CN-MI additive has lowest potential plateau and highest starting point of lithium ion insertion process (1.6 V), followed by F-MI (1.5 V), O-MI (1.24 V), and blank electrolyte (0.91 V). It is obviously ascribed to the reduction of the electrolyte systems (solvent and additive) to form SEI layer in accordance to CV results. In addition, it also indicates that the kinetics of intercalation/de-intercalation lithium ion for CN-MI electrolyte additive is much faster compared with three other kinds of electrolyte systems. In other words, it can be concluded that the presence of the electronegativity functional group (F and CN) on MI-based electrolyte additive

can suppress the decomposition of the electrolyte system, improve the formation of SEI layer and also able to facilitate a faster intercalation/de-intercalation of lithium ion into the graphite anode.

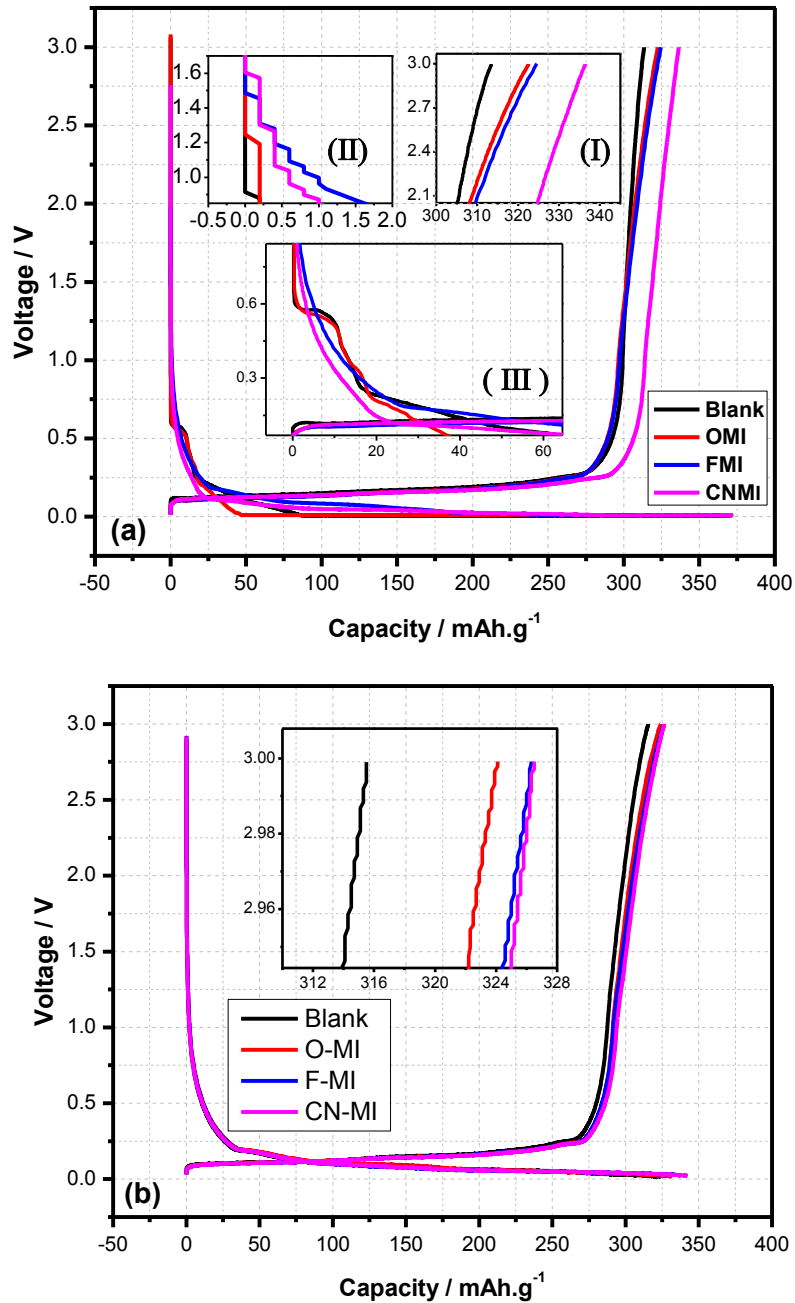


Figure 4.7: Charge and discharge profile of MCMB/Li half-cell with and without additives under 0.1 C-Rate at the room temperature and potential range 0-3 V vs Li/Li⁺, (a) 1st cycle (b) 2nd cycle

Figure 4.7 (b) shows the second charge discharge processes. From this figure, it can be seen that the slowly sloping line occur in all of kinds of electrolyte system. It indicated that the further electrolyte decomposition can be prevented by SEI layer that has been formed in the first cycle. The second charge and discharge curve shows that the electrolyte with the CN-MI additive still provide the highest discharge capacity (326.5 mAh/g), followed by electrolyte with F-MI additive (326.3 mAh/g), electrolyte with O-MI additive (324.1 mAh/g), and the blank electrolyte (315.5 mAh/g), respectively. It means that the addition MI-based additive into electrolyte system not only can improve electrochemical performance of the battery, but also can enhance the battery capacity.

4.2.2.2 Cycle-ability Profile on MCMB/Li half cell

Figure 4.8 shows the cycle-ability performance of MCMB/Li⁺ half-cell. The capacity retention of MCMB/Li⁺ half-cell with CN-MI additive for the first tenth cycles showed superior capacity compared to other electrolyte systems. From Fig 4.8 shows the discharge capacity is 2.1% (O-MI), 7.1% (F-MI), and 11.7% (CN-MI) greater than the electrolyte without additives after 10 cycles. It suggests that the CN-MI and F-MI additive is able to form a stable SEI layer and enhances the cycling performance of the battery. In contrast, the lowest capacity at the blank electrolyte systems during cycles suggesting that the poor passivation of the electrode surface in the blank system. It believed that by adding the electronegativity functional groups (F and CN) into MI-based additives can produce an effective SEI layer and enhance the battery performance. This result is consistent and similar with the evidence in CV and EIS results.

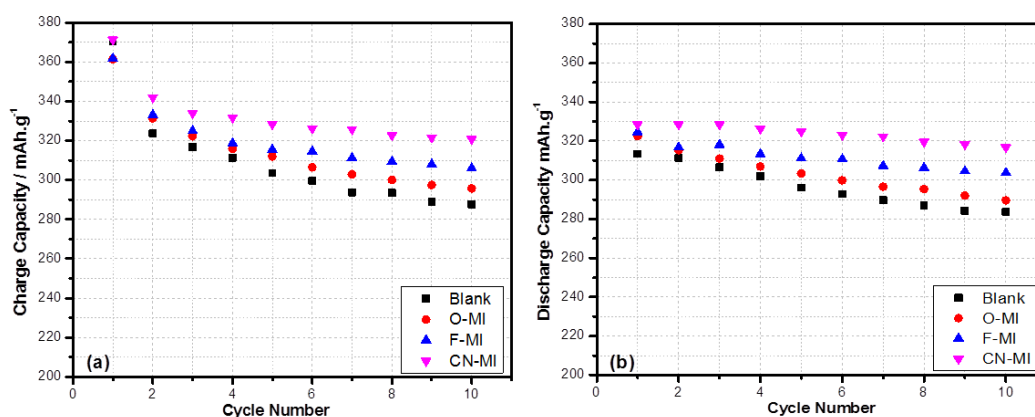


Figure 4.8: Comparison of cycle-ability of MCMB/Li half-cell with and without additives in electrolyte under 0.1 C-rate at room temperature and potential range 0-3 V vs Li/Li⁺, (a) charge (b) discharge capacity

4.2.2.3 Charge Discharge Profile on MCMB/LiCoO₂ full cell

The addition of the MI-based additives (O-MI, F-MI, and CN-MI) into the electrolyte also can improve the performance of the MCMB/LiCoO₂ full-cell system. Fig 4.9 shows the first charge discharge curve using fourth kind of electrolyte systems. In the first charge discharge processes (Fig 4.9), the cell with the blank electrolyte provides the lowest discharge capacity (141.08 mAh/g) and lowest reversible capability (86.08%). The capacity gradually increases after adding MI-based additives into the electrolyte, i.e. the discharge capacity and reversibility of the cell with O-MI additive is 145.87 mAh/g (3.4% increase Vs blank) and 89.74%, respectively. The discharge capacity and reversibility of the full-cell system with F-MI additive is 149 mAh/g (5.6% increase Vs blank) and 92.56%, respectively. Meanwhile, the cell containing F-MI additive provides the highest discharge capacity (152.78 mAh/g) and highest reversible capability (94.85%). Thus, it can be concluded that the cell containing MI-based additives show a better performance on MCMB/LiCoO₂ full-cell when they compared with the blank electrolyte cell system. In contrast with MCMB/Li⁺ half-cell, the performance of MCMB/LiCoO₂ full-cell containing F-MI additive has significantly improved, indicating that the F-MI additive more compatible to be applied on the full-cell system than the half-cell system.

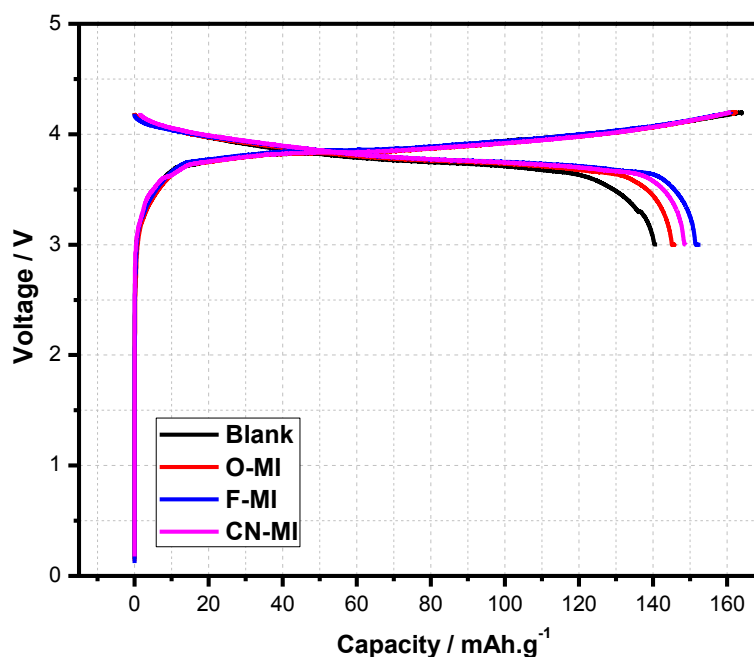


Figure 4.9: Charge and discharge profile of MCMB/LiCoO₂ full-cell with and without additives at 1st cycle under 0.1 C-Rate at the room temperature and potential range 3 - 4.2V vs Li/Li⁺.

4.2.2.4 Cycle-ability Profile on MCMB/LiCoO₂ full cell

Fig 4.10 shows the significant improvement in cycle-ability on MCMB/LiCoO₂ full-cell system after addition of F-MI additive in several cycles with different scan rate. As mentioned above the cell with F-MI additive provides the highest charge/discharge capacity and highest reversible capability compare to other electrolyte system. The cell with CN-MI additive has slightly lower discharge capacity, followed by the cell with O-MI additive and blank electrolyte. Interestingly at the first tenth cycles, the capacity retention of the cells with CN-MI additive during 0.1C rate shows a little bit higher charge/discharge capability compared with O-MI additive. However, during 0.2 C rate battery formation, the cells with CN-MI additive has slightly lower discharge capacity than O-MI additive in the next tenth cycles. Meanwhile, the most capacity loss during cycling occurs with the cell containing blank electrolyte. From these results, it also can be seen that F-MI additive, not only enhances battery capacity, but also increases high power density, compared to other electrolyte system. There are several factors cause cycle-ability in the lithium battery to gradually decay, e.g. further

electrolyte decomposition, increases the thickness of the SEI layer and charge transfer resistance, and degradation of the electrode material.

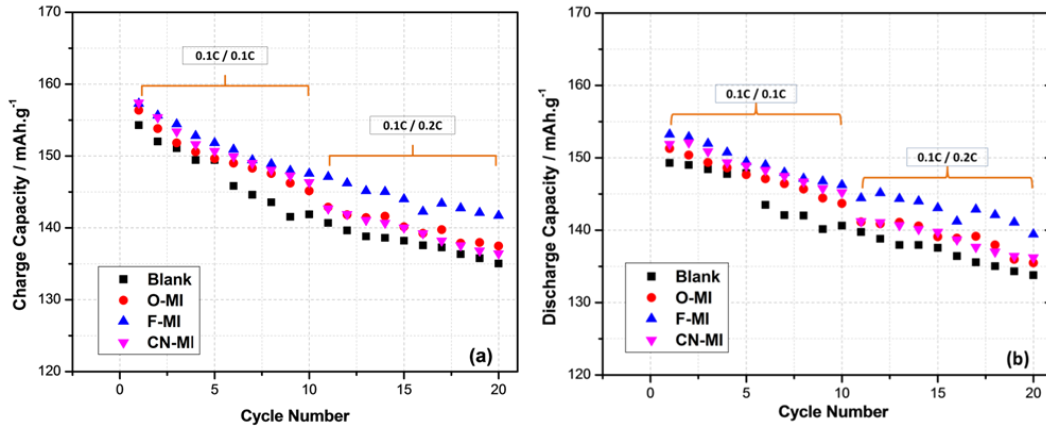


Figure 4.10: Comparison of cycle-ability of MCMB/LiCoO₂ full-cell with and without additives until 20th cycles at room temperature and potential range 3 - 4.2V vs Li/Li⁺, (a) charge (b) discharge capacity

4.2.2.5 Rate Capability Profile on MCMB/LiCoO₂ full cell

Fig 4.11 investigates the rate capability performance of the MCMB/LiCoO₂ full-cell with and without additives at room temperature and potential range 3 - 4.2 V vs Li/Li⁺. The battery energy density using F-MI additive reaches the highest discharge capacity value at any rate (0.1, 0.2, 0.3 0.5, 1, and 2 C), followed by the cell with CN-MI additive, commercial product (O-MI additive), and without any additive (blank electrolyte). These results correspond with the evidence shown on impedance results of SEI layer resistance and the charge transfer resistance of active materials. This result also concordance to the warburg coefficient which is related to rate capability. The presence of MI-based additives is believed to facilitate a better SEI formation and enhance the battery performance.

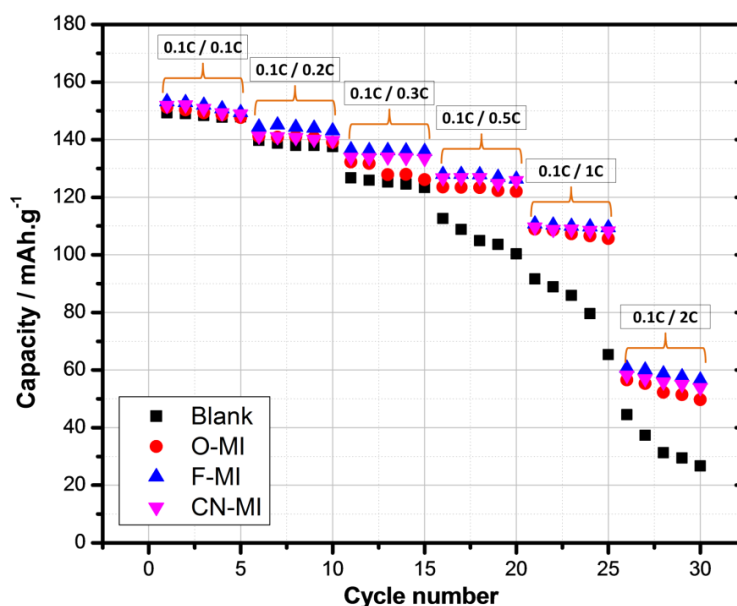


Figure 4.11: Rate capability of MCMB/LiCoO₂ full-cell with and without additives at room temperature and potential range 3 - 4.2V vs Li/Li⁺

4.2.3 Electrochemical Impedance Spectroscopy (EIS) test

EIS is one of the most powerful tools to analyze electrochemical processes occurring at electrode/electrolyte interfaces, and has been widely applied to the analysis of electrochemical lithium intercalation into carbonaceous materials including graphite (Xu, Zhuang et al. 2013). EIS measurements usually were performed on the graphite electrode during the process of the first lithium ion insertion (in situ conservation). However, the EIS also can be performed on the graphite electrode after cycling process (ex situ conservation). EIS is unique in that it requires only small amplitude variations in an externally-defined potential to obtain high precision measurements for surface characterization and the interpretation of interfacial phenomena (Wang and Rick 2014). The physical and chemical characteristics of an electrode's surface can be evaluated by alternating current (AC) circuit theory, to allow an interpretation of effect of variables such as resistance, capacitance, and conductance.

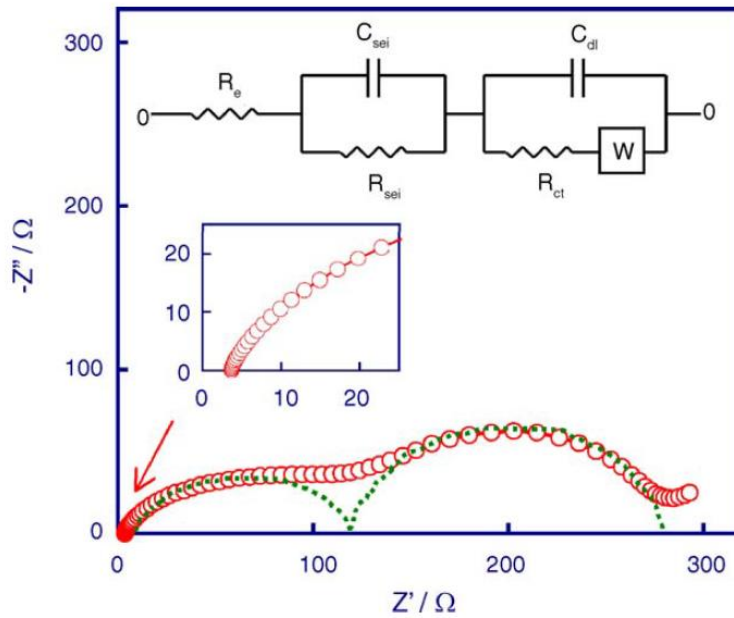


Figure 4.12: Equivalent-circuit for the EIS of Li/graphite cell. The EIS was recorded at 0.05V (Zhang, Xu et al. 2006)

EIS results shown in Fig. 4.12 represent the internal battery construction, which is divided into four items. The first resistance (R_1) represents electrolyte resistance or ionic conductivity, the first RC circuit represents the bulk of SEI layer, and the second RC circuit represents contact resistance between SEI and electrode surface, while the last Warburg element (W_1) connects in series to the diffusion resistance of the electrodes, typically representing the cathode (Zhang, Xu et al. 2006).

4.2.3.1 EIS Test on MCMB/Li half cell

Figure 4.13 shows the EIS measurements for a Li/MCMB anode half-cell using four types of electrolyte additives after tenth cycle battery formation. From impedance spectra, the first depressed high frequency semicircle differ has generally been believed that is related to the SEI layer (R_{sei}), and the second depressed medium frequency differ is related to the charge transfer resistance (R_{ct}) on both cathode and anode (Wang, Appleby et al. 2001).

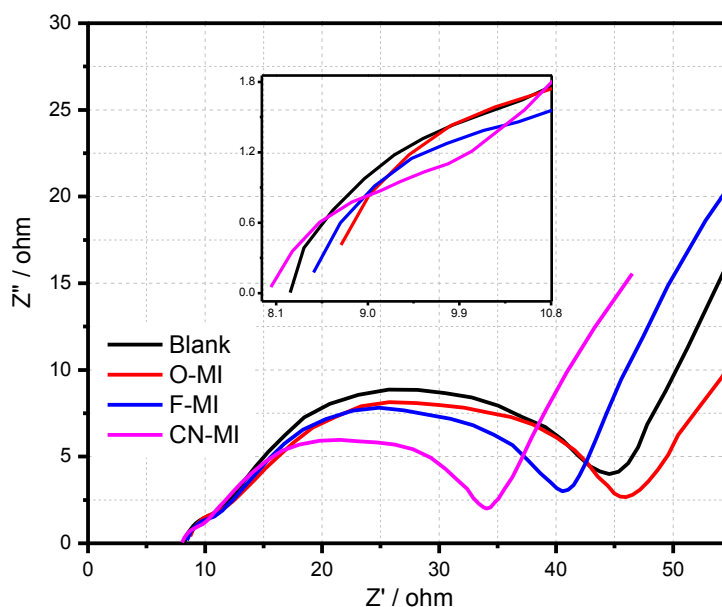
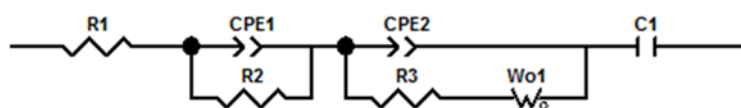


Figure 4.13: Impedance Spectra of MCMB/Li half-cell after tenth cycle with 1 M LiPF_6 and EC:PC:DEC (3:2:5 v/v) electrolyte system.

Table 4.2: Electrode kinetic parameters obtained from equivalent circuit fitting of experimental data with various electrolytes on MCMB/Li half-cell.



Electrolyte	R_1/R_e	R_2/R_{sei}	R_3/R_{ct}	W_0	R_{total}
Blank	7.90	5.9	31.65	0.85	46.305
O-MI	8.10	4.8	32.15	0.75	45.80
F-MI	8.05	4.9	28.35	0.63	41.93
CN-MI	7.80	3.5	21.65	0.59	33.54

According to Fig 4.13 and Table 4.2, all of kinds of electrolyte have similar electrolyte resistance (R_1), indicating that the adding MI additive into electrolyte system does not substantially change the ionic conductivity of the electrolyte system. However, the value of bulk SEI layer resistance (R_2), charge transfer resistance (R_3), and Warburg resistance (W_0) varies greatly with the addition of MI. The cell with the CN-MI additive shows the smallest R_2 (3.5Ω), followed by the cell with O-MI additive (4.8Ω), F-MI additive (4.9Ω), and blank

electrolyte (5.9 Ω) respectively. It is indicated that the SEI formed with the MI-based electrolyte additive is more compact and has a lowest resistance (especially maleimide additive with cyano group as substituent).

The cell with the CN-MI additive also shows the smallest R_3 and W_o (21.65 Ω and 0.59 Ω), followed by the cell with F-MI additive (28.35 Ω and 0.63 Ω), O-MI additive (32.15 Ω and 0.75 Ω), and blank electrolyte (31.65 Ω and 0.85 Ω). As described above that R_3 is related to the charge transfer resistance between SEI layer and interface of the electrode and W_o is related to the ionic diffusion resistance of the bulk cathode. Additionally, the smallest total resistance (R_{total}) also was obtained at the cell with CN-MI additive, followed by the cell with F-MI additive, O-MI additive, and Blank, respectively. Thus, it is indicated that by adding molecule with high electronegativity and high electron withdrawing group (F and CN) into MI-based electrolyte additives can provide an excellent ionic diffusivity and also can increase the electrochemical performance of LIBs.

4.2.3.2 EIS Test on MCMB/LiCoO₂ full cell

Figure 4.14 shows the EIS measurements for a MCMB/LiCoO₂ full-cell using four types of electrolyte additives after tenth cycle battery formation. Table 4.3 shows electrode kinetic parameters obtained from equivalent circuit fitting of experimental data with various electrolytes. The cell with F-MI additive provides the lowest total resistance (99.185 Ω), followed by CN-MI (110.23 Ω), O-MI (113.625 Ω), and blank electrolyte (119.745 Ω). Similar with MCMB/Li half-cell, all of kinds of electrolyte have similar electrolyte resistance (R_1), indicating that the adding MI additive into electrolyte system does not substantially change the ionic conductivity of the electrolyte system. However, the value of bulk SEI layer resistance (R_2), charge transfer resistance (R_3), and Warburg resistance (W_o) varies greatly with the addition of MI-based additives (see Table 4.3). In contrast with MCMB/Li⁺ half-cell, the EIS result of MCMB/LiCoO₂ full-cell containing F-MI shows the smallest SEI layer resistance (R_2/R_{sei}), charge transfer resistance (R_3/R_{ct}), and Warburg resistance (W_o), indicating that the SEI formed with the F-MI additive is more compact to give the lowest resistance and provide excellent electrochemical performance. These results correspond with the evidence shown

on the charge discharge analysis. Thus, it can be concluded that F-MI is the most appropriate MI-based additives to enhance the battery performance, especially on MCMB/LiCoO₂ full-cell system.

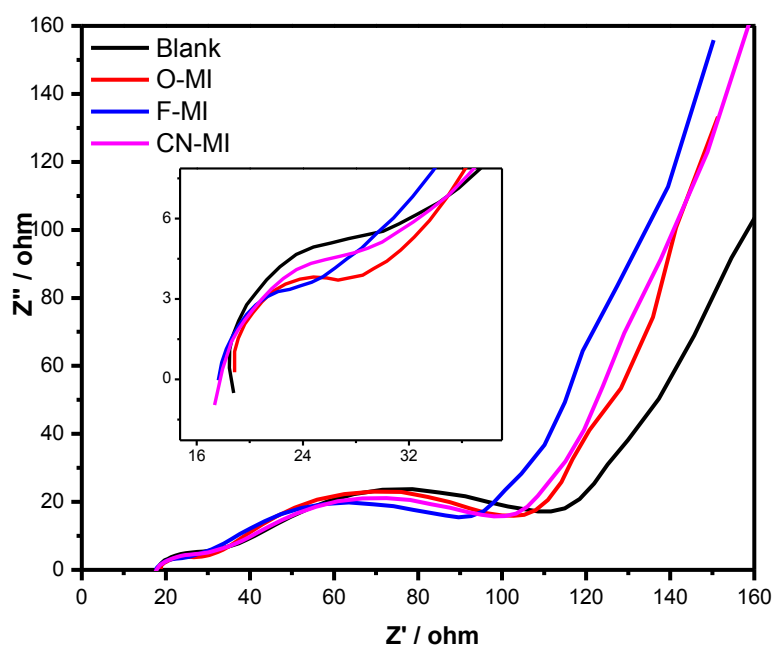
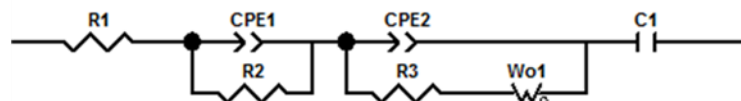


Figure 4.14: Impedance Spectra of MCMB/LiCoO₂ full-cell after tenth cycle with 1 M LiPF₆ and EC:EMC (1:1 v/v) electrolyte system.

Table 4.3: Electrode kinetic parameters obtained from equivalent circuit fitting of experimental data with various electrolytes on MCMB/LiCoO₂ full cell.



Electrolyte	R_1/R_e	R_2/R_{sei}	R_3/R_{ct}	W_o	R_{total}
Blank	17.35	15.05	87	0.345	119.745
O-MI	17.85	11.50	84	0.275	113.625
F-MI	17.50	9.50	72	0.185	99.185
CN-MI	17.25	11.75	81	0.230	110.230

4.3 SEI Evaluation

SEM analysis was performed to understand the effect of the electrolyte additive addition on the morphology of the MCMB electrode. According to the theory of the solid electrolyte interface (SEI) layers formation, most of the SEI layer formed on the graphite anode as a result decomposition of the electrolyte components (solvent and salt), and mainly during the first cycle. These decomposition products undergo a precipitation process and begin forming the SEI layer until all the sites on the graphite surface are covered. The presence of the SEI layer can enhance the capacity and stability of the anode graphite. In this study, the SEI formation is highly affected by the presence of electrolyte additive. The SEI effect on the battery's performance has been discussed in the previous chapter which gives a significant contribution to the increase in performance. In this chapter the SEI formation will be evaluated in detail by scanning electron microscopy (SEM) and energy dispersive X-ray spectroscopy (EDX).

4.3.1 SEM Result

Figure 4.15 show SEM images that obtained from MCMB for lithium-ion batteries before electrochemical cycling for comparison. While Fig 4.16 show SEM images obtained from MCMB after the tenth cycles. The insets of Fig. 4.15 and Fig. 4.16 (a-d) show SEM images of MCMB at x3000 magnification. Figure 4.16 (a-d) show that the shape of MCMB particles after tenth cycles in cells with 1M LiPF₆/EC:PC:DEC (without and with MI-based additive) was clearly changed and become an indistinct surface when its compared with the MCMB before electrochemical cycling (Fig. 4.15). It indicates that the surface of MCMB after tenth cycles was covered with a thin passivation layer which in this case is suspected as a SEI layer that formed from solvent decomposition and lithium ion co-intercalation during tenth cycles. Additionally, from the insets of Fig 4.16 (a), it can be seen that the surface of MCMB without any additive is rough and porous which indicates that the SEI layer formed on the anode surface is disordered, incompact, and causing a thicker layer. Meanwhile, the roughness and the thickness of the MCMB surface gradually decreased with the addition of MI-based additives into the electrolyte system as shown in the insets of Fig. 4.16 (b) (O-MI), Fig.

4.16 (c) (F-MI), and Fig. 4.16 (d) (CN-MI), respectively. Thus, it can be concluded that by adding molecule with high electronegativity and high electron withdrawing group (F and CN) into MI-based electrolyte additives can make the formation of SEI layer more smooth, thinner, compact, and effective.

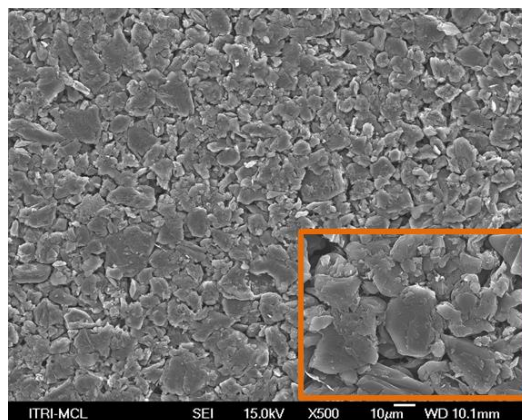


Figure 4.15: SEM image of MCMB before electrochemical cycling (x500). Inset shows image at x3000 magnification.

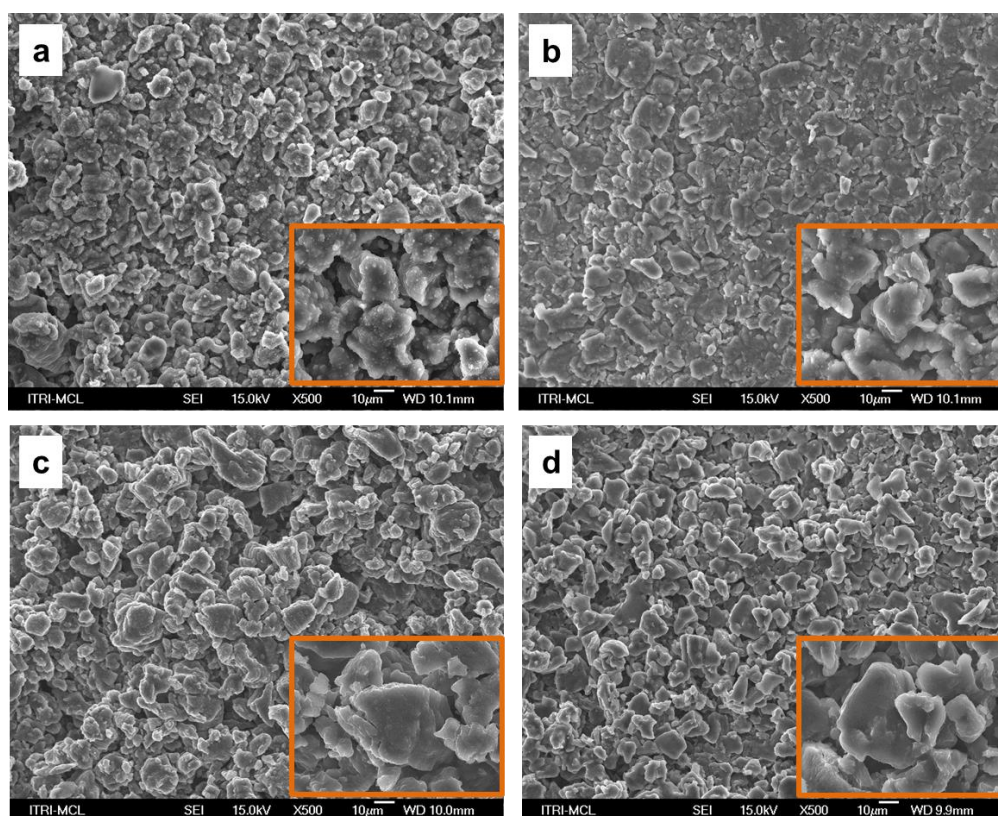


Figure 4.16: SEM image of MCMB/Li half cell after the tenth cycles (x500) in cell with additive electrolyte (a) Blank, (b) O-MI, (c) F-MI and (d) CN-MI. Inset shows image at x3000 magnification.

4.3.2 EDX Result

To better understand the chemical composition of the SEI formed on the MCMB anode surface in cells with 1M LiPF₆/EC:PC:DEC (without and with MI-based additive), the MCMB anode surface after tenth cycles was analyzed with EDX. The EDX spectrum of the MCMB anode surface was depicted in Fig 4.17 (a-d). The spectrum is taken on the same area of the entire MCMB anode surface, with and without additives. Carbon (C) can be present as the carbon content of graphite anode and also present as part of R-CH₂-OCO₂Li, polymerization of MI-based additive and (CH₂OCO₂Li)₂ as organic SEI components. Meanwhile, inorganic SEI components, such as Li₂O, Li₂CO₃ formed from oxygen elements (O), LiF and Li_xPF_y and Li_xPO_yF_z formed from fluorine (F) and phosphorus (P) elements can inhibit ionic diffusion, intercalation and de-intercalation of lithium ions, and eventually lead to the performance decay of LIBs.

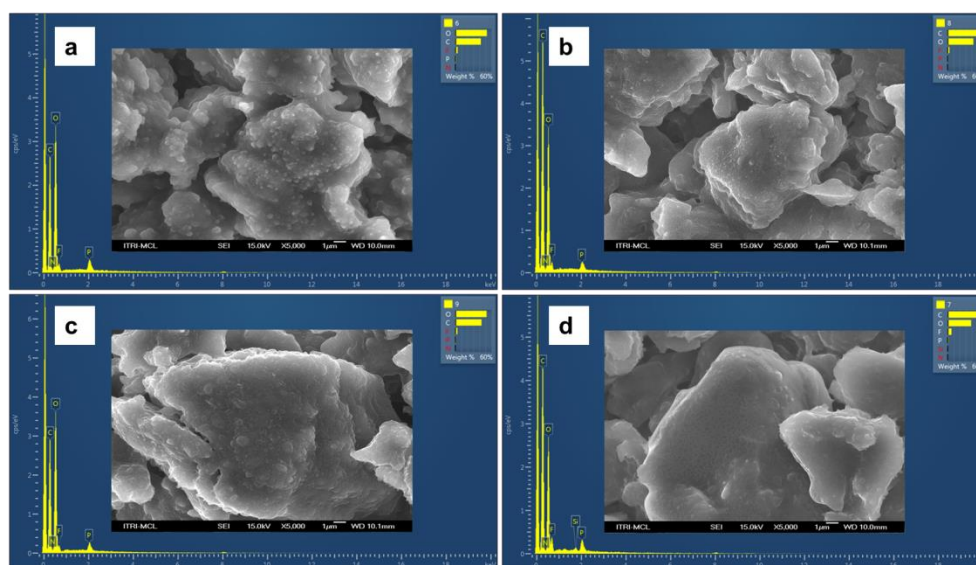


Figure 4.17: EDX profile of MCMB/Li half-cell after the tenth cycles in cell with additive electrolyte (a) Blank, (b) O-MI, (c) F-MI and (d) CN-MI. Inset shows image at x5000 magnification.

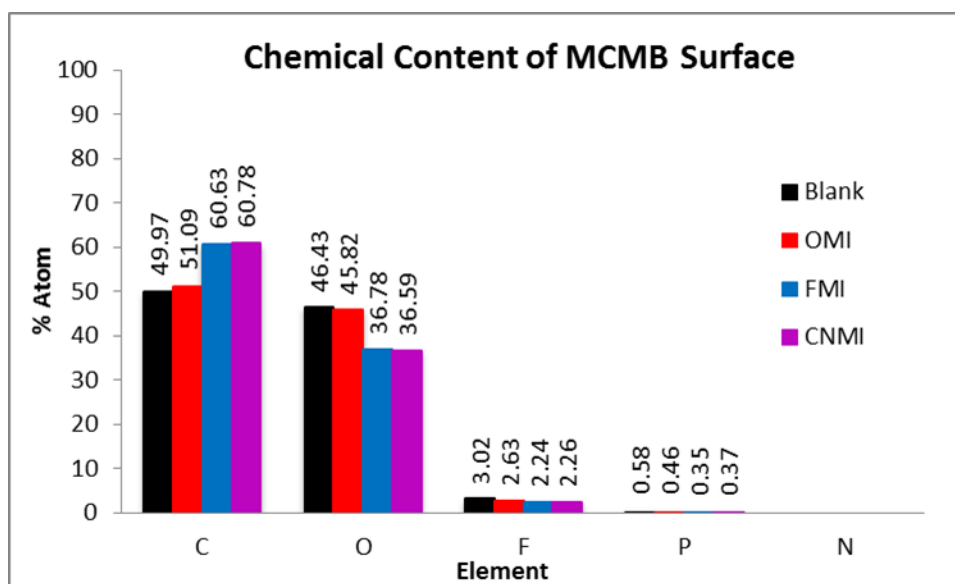


Figure 4.18: Graphic of chemical content of MCMB surface selected regarding EDX profile of variant MCMB with electrolyte additive.

Based on the EDX result at Fig 4.17 and Fig 4.18, it can be seen that the MCMB surface with CN-MI electrolyte additive has the lowest oxygen content (O) and the highest carbon content (C) compared with the F-MI, O-MI and blank additive. It means that the MCMB surface with CN-MI electrolyte additive provides highest organic SEI part followed by MCMB surface with F-MI, O-MI and blank additive. While in contrast, the MCMB surface with a blank electrolyte provides the highest inorganic SEI components as evidenced from the highest contents of O, F, and P elements.

“This page intentionally left blank”

CHAPTER V

CONCLUSION

This study evaluates the electronegativity functional group effects on maleimide-based electrolyte additives to the SEI formation and the battery performance. The new maleimide-based additives, namely 4-fluoro-o-phenylenedimaleimide (F-MI) and 4-cyano-o-phenylenedimaleimide (CN-MI) have been successfully synthesized. The SEI layer formation in four electrolyte systems, including blank electrolyte, commercial product (O-MI), F-MI, and CN-MI were investigated by electrochemical related measurements. The morphology and chemical composition of the SEI layer are also measured by surface electron morphology (SEM) and energy dispersive X-ray spectroscopy (EDX).

In comparison with the blank electrolyte, the additives (O-MI, F-MI, and CN-MI) show higher electrochemical stability and higher reversibility capability. The electrolyte containing MI based additives is able to trigger SEI layer formation on anode's surface in which the SEI forms within higher reduction potential. In addition, the electronegativity substitution additives, F-MI and CN-MI are used to produce a thinner, smooth, unique and more compact SEI layer to give a lower resistance, as shown in EIS, SEM, and EDX results. Furthermore, F-MI and CN-MI additive also shows the excellent performance on MCMB/Li⁺ half-cell. Interestingly, the CN-MI additive provides the highest reversible capability at the first cycle and excellent durability until the tenth cycles. We believe stronger electron withdrawing substitution may attract electron on lower LUMO, which decreases the energy band gap to early reduce on anode surface. Fluoro and cyano functional groups are used to fabricate a specific composition of SEI. In terms of our results, this SEI forms CN-MI is unique and prompt highly diffusivity of lithium ion, which enhances battery performance. Our results show that F-MI and CN-MI additives are the most suitable additives due to its excellent SEI formation and battery performance enhancement compares with blank electrolyte and commercial product (O-MI).

“This page intentionally left blank”

REFERENCE

- Agubra, V. A. and J. W. Fergus (2014). "The formation and stability of the solid electrolyte interface on the graphite anode." *Journal of Power Sources* **268**: 153-162.
- An, S. J., J. Li, C. Daniel, D. Mohanty, S. Nagpure and D. L. Wood (2016). "The state of understanding of the lithium-ion-battery graphite solid electrolyte interphase (SEI) and its relationship to formation cycling." *Carbon* **105**: 52-76.
- Chai, S., S.-H. Wen and K.-L. Han (2011). "Understanding electron-withdrawing substituent effect on structural, electronic and charge transport properties of perylene bisimide derivatives." *Organic electronics* **12**(11): 1806-1814.
- Chattopadhyay, S., A. L. Lipson, H. J. Karmel, J. D. Emery, T. T. Fister, P. A. Fenter, M. C. Hersam and M. J. Bedzyk (2012). "In situ X-ray study of the solid electrolyte interphase (SEI) formation on graphene as a model Li-ion battery anode." *Chemistry of Materials* **24**(15): 3038-3043.
- Cheng, C.-S., F.-M. Wang and J. Rick (2012). "Aqueous Additive for Lithium Ion Batteries: Promotes Novel Solid Electrolyte Interface (SEI) Layer with Overall Cost Reduction." *Int. J. Electrochem. Sci* **7**: 8676-8687.
- Choi, N. S., Z. Chen, S. A. Freunberger, X. Ji, Y. K. Sun, K. Amine, G. Yushin, L. F. Nazar, J. Cho and P. G. Bruce (2012). "Challenges Facing Lithium Batteries and Electrical Double-Layer Capacitors." *Angewandte Chemie International Edition* **51**(40): 9994-10024.
- Cresce, A. v., S. M. Russell, D. R. Baker, K. J. Gaskell and K. Xu (2014). "In situ and quantitative characterization of solid electrolyte interphases." *Nano letters* **14**(3): 1405-1412.
- Doeff, M. M. (2013). Battery Cathodes. *Batteries for Sustainability*, Springer: 5-49.
- Fergus, J. W. (2010). "Recent developments in cathode materials for lithium ion batteries." *Journal of Power Sources* **195**(4): 939-954.
- Fu, L., H. Liu, C. Li, Y. P. Wu, E. Rahm, R. Holze and H. Wu (2006). "Surface modifications of electrode materials for lithium ion batteries." *Solid State Sciences* **8**(2): 113-128.
- Ghandi, K. (2014). "A review of ionic liquids, their limits and applications." *Green and Sustainable Chemistry*.
- Goriparti, S., E. Miele, F. De Angelis, E. Di Fabrizio, R. P. Zaccaria and C. Capiglia (2014). "Review on recent progress of nanostructured anode materials for Li-ion batteries." *Journal of Power Sources* **257**: 421-443.
- Hamidah, N. L. (2013). "Synthesis of fluorine functional group of maleimide based additive and its applications to the solid electrolyte interface (SEI) formation of lithium ion battery." National Taiwan University of Science and Technology: 1-155.
- Haregewoin, A. M., E. G. Leggesse, J.-C. Jiang, F.-M. Wang, B.-J. Hwang and S. D. Lin (2014). "Comparative study on the solid electrolyte interface formation by the reduction of alkyl carbonates in lithium ion battery."

- Electrochimica Acta* **136**: 274-285.
- Haregewoin, A. M., A. S. Wotango and B.-J. Hwang (2016). "Electrolyte additives for lithium ion battery electrodes: progress and perspectives." *Energy & Environmental Science* **9**(6): 1955-1988.
- Hu, Y., W. Kong, Z. Wang, X. Huang and L. Chen (2005). "Tetrachloroethylene as new film-forming additive to propylene carbonate-based electrolytes for lithium ion batteries with graphitic anode." *Solid State Ionics* **176**(1): 53-56.
- Jeong, G., Y.-U. Kim, H. Kim, Y.-J. Kim and H.-J. Sohn (2011). "Prospective materials and applications for Li secondary batteries." *Energy & Environmental Science* **4**(6): 1986-2002.
- Julien, C. M., A. Mauger, K. Zaghib and H. Groult (2014). "Comparative issues of cathode materials for Li-ion batteries." *Inorganics* **2**(1): 132-154.
- Jung, H. M., S.-H. Park, J. Jeon, Y. Choi, S. Yoon, J.-J. Cho, S. Oh, S. Kang, Y.-K. Han and H. Lee (2013). "Fluoropropane sultone as an SEI-forming additive that outperforms vinylene carbonate." *Journal of Materials Chemistry A* **1**(38): 11975-11981.
- Korepp, C., H. Santner, T. Fujii, M. Ue, J. Besenhard, K.-C. Möller and M. Winter (2006). "2-Cyanofuran—A novel vinylene electrolyte additive for PC-based electrolytes in lithium-ion batteries." *Journal of power sources* **158**(1): 578-582.
- Lee, H., M. Yanilmaz, O. Toprakci, K. Fu and X. Zhang (2014). "A review of recent developments in membrane separators for rechargeable lithium-ion batteries." *Energy & Environmental Science* **7**(12): 3857-3886.
- Malmgren, S., K. Ciosek, M. Hahlin, T. Gustafsson, M. Gorgoi, H. Rensmo and K. Edström (2013). "Comparing anode and cathode electrode/electrolyte interface composition and morphology using soft and hard X-ray photoelectron spectroscopy." *Electrochimica Acta* **97**: 23-32.
- Marcinek, M., J. Syzdek, M. Marczewski, M. Piszcz, L. Niedzicki, M. Kalita, A. Plewa-Marczewska, A. Bitner, P. Wiczorek and T. Trzeciak (2015). "Electrolytes for Li-ion transport—Review." *Solid State Ionics* **276**: 107-126.
- Nie, M. and B. L. Lucht (2014). "Role of lithium salt on solid electrolyte interface (SEI) formation and structure in lithium ion batteries." *Journal of The Electrochemical Society* **161**(6): A1001-A1006.
- Park, M., X. Zhang, M. Chung, G. B. Less and A. M. Sastry (2010). "A review of conduction phenomena in Li-ion batteries." *Journal of Power Sources* **195**(24): 7904-7929.
- Park, Y., S. H. Shin, H. Hwang, S. M. Lee, S. P. Kim, H. C. Choi and Y. M. Jung (2014). "Investigation of solid electrolyte interface (SEI) film on LiCoO₂ cathode in fluoroethylene carbonate (FEC)-containing electrolyte by 2D correlation X-ray photoelectron spectroscopy (XPS)." *Journal of Molecular Structure* **1069**: 157-163.
- Radvanyi, E., K. Van Havenbergh, W. Porcher, S. Jouanneau, J.-S. Bridel, S. Put and S. Franger (2014). "Study and modeling of the Solid Electrolyte Interphase behavior on nano-silicon anodes by Electrochemical Impedance Spectroscopy." *Electrochimica Acta* **137**: 751-757.
- Santner, H., K.-C. Möller, J. Ivančo, M. Ramsey, F. Netzer, S. Yamaguchi, J. Besenhard and M. Winter (2003). "Acrylic acid nitrile, a film-forming

- electrolyte component for lithium-ion batteries, which belongs to the family of additives containing vinyl groups." *Journal of power sources* **119**: 368-372.
- Shi, F., P. N. Ross, H. Zhao, G. Liu, G. A. Somorjai and K. Komvopoulos (2015). "A Catalytic Path for Electrolyte Reduction in Lithium-Ion Cells Revealed by in Situ Attenuated Total Reflection-Fourier Transform Infrared Spectroscopy." *Journal of the American Chemical Society* **137**(9): 3181-3184.
- Shi, F., H. Zhao, G. Liu, P. N. Ross, G. A. Somorjai and K. Komvopoulos (2014). "Identification of Diethyl 2, 5-Dioxahexane Dicarboxylate and Polyethylene Carbonate as Decomposition Products of Ethylene Carbonate Based Electrolytes by Fourier Transform Infrared Spectroscopy." *The Journal of Physical Chemistry C* **118**(27): 14732-14738.
- Shkrob, I. A., Y. Zhu, T. W. Marin and D. Abraham (2013). "Reduction of carbonate electrolytes and the formation of solid-electrolyte interface (SEI) in Lithium-ion batteries. 1. spectroscopic observations of radical intermediates generated in one-electron reduction of carbonates." *The Journal of Physical Chemistry C* **117**(38): 19255-19269.
- Song, J., Y. Wang and C. Wan (1999). "Review of gel-type polymer electrolytes for lithium-ion batteries." *Journal of Power Sources* **77**(2): 183-197.
- Soto, F. A., Y. Ma, J. M. Martinez de la Hoz, J. M. Seminario and P. B. Balbuena (2015). "Formation and growth mechanisms of solid-electrolyte interphase layers in rechargeable batteries." *Chemistry of Materials* **27**(23): 7990-8000.
- Stephan, A. M. (2006). "Review on gel polymer electrolytes for lithium batteries." *European Polymer Journal* **42**(1): 21-42.
- Torres, W., L. Cantoni, A. Tesio, M. Del Pozo and E. Calvo (2015). "EQCM study of oxygen cathodes in DMSO LiPF₆ electrolyte." *Journal of Electroanalytical Chemistry*.
- Tsai, W.-Y., P.-L. Taberna and P. Simon (2014). "Electrochemical quartz crystal microbalance (EQCM) study of ion dynamics in nanoporous carbons." *Journal of the American Chemical Society* **136**(24): 8722-8728.
- Verma, P., P. Maire and P. Novák (2010). "A review of the features and analyses of the solid electrolyte interphase in Li-ion batteries." *Electrochimica Acta* **55**(22): 6332-6341.
- Wang, C., A. J. Appleby and F. E. Little (2001). "Electrochemical impedance study of initial lithium ion intercalation into graphite powders." *Electrochimica acta* **46**(12): 1793-1813.
- Wang, F.-M., H.-M. Cheng, H.-C. Wu, S.-Y. Chu, C.-S. Cheng and C.-R. Yang (2009). "Novel SEI formation of maleimide-based additives and its improvement of capability and cyclicability in lithium ion batteries." *Electrochimica Acta* **54**(12): 3344-3351.
- Wang, F.-M. and J. Rick (2014). "Synergy of Nyquist and Bode electrochemical impedance spectroscopy studies to commercial type lithium ion batteries." *Solid State Ionics* **268**: 31-34.
- Wang, F.-M., M.-H. Yu, C.-S. Cheng, S. A. Pradanawati, S.-C. Lo and J. Rick (2013). "Phenylenedimaleimide positional isomers used as lithium ion battery electrolyte additives: Relating physical and electrochemical

- characterization to battery performance." *Journal of Power Sources* **231**: 18-22.
- Whittingham, M. S. (2004). "Lithium batteries and cathode materials." *Chemical reviews* **104**(10): 4271-4302.
- Wu, Y.-P., E. Rahm and R. Holze (2003). "Carbon anode materials for lithium ion batteries." *Journal of Power Sources* **114**(2): 228-236.
- Xu, J., S. Dou, H. Liu and L. Dai (2013). "Cathode materials for next generation lithium ion batteries." *Nano Energy* **2**(4): 439-442.
- Xu, K. (2010). "Electrolytes and interphasial chemistry in Li ion devices." *Energies* **3**(1): 135-154.
- Xu, S.-D., Q.-C. Zhuang, J. Wang, Y.-Q. Xu and Y.-B. Zhu (2013). "New Insight into Vinylethylene Carbonate as a Film Forming Additive to Ethylene Carbonate-Based Electrolytes for Lithium-Ion Batteries." *Int. J. Electrochem. Sci* **8**: 8058-8076.
- Zhang, L., J. Huang, K. Youssef, P. C. Redfern, L. A. Curtiss, K. Amine and Z. Zhang (2014). "Molecular Engineering toward Stabilized Interface: An Electrolyte Additive for High-Performance Li-Ion Battery." *Journal of The Electrochemical Society* **161**(14): A2262-A2267.
- Zhang, S., M. S. Ding, K. Xu, J. Allen and T. R. Jow (2001). "Understanding solid electrolyte interface film formation on graphite electrodes." *Electrochemical and Solid-State Letters* **4**(12): A206-A208.
- Zhang, S., K. Xu and T. Jow (2006). "EIS study on the formation of solid electrolyte interface in Li-ion battery." *Electrochimica acta* **51**(8): 1636-1640.
- Zhang, S. S. (2006). "A review on electrolyte additives for lithium-ion batteries." *Journal of Power Sources* **162**(2): 1379-1394.
- Zhang, S. S. (2007). "Electrochemical study of the formation of a solid electrolyte interface on graphite in a LiBC₂O₄F₂-based electrolyte." *Journal of Power Sources* **163**(2): 713-718.